Title: Two specific populations of GABAergic neurons originating from the medial and the caudal ganglionic eminences aid in proper navigation of callosal axons.
Authors: Niquille M, Minocha S, Hornung JP, Rufer N, Valloton D, Kessaris N, Alfonsi F, Vitalis T, Yanagawa Y, Devenoges C, Dayer A, Lebrand C
Journal: Developmental neurobiology
Year: 2013 Sep
Volume: 73
Issue: 9
Pages: 647-72
DOI: 10.1002/dneu.22075

Two specific populations of GABAergic neurons originating from the medial and the caudal ganglionic eminences aid in proper navigation of callosal axons

Mathieu Niquille [1,*], Shilpi Minocha [1,*], Jean-Pierre Hornung [1], Nathalie Rufer [2], Delphine Valloton[1], Nicoletta Kessaris [3], Fabienne Alfonsi [3], Tania Vitalis [4], Yuchio Yanagawa [5], Christiane Devenoges [1], Alexandre Dayer [6, 7, 8] and Cécile Lebrand [1, #].

[1] Département des neurosciences fondamentales, University of Lausanne, Rue du Bugnon 9, CH-1005 Lausanne, Switzerland.

[2] Department of Research, University Hospital Centre and University of Lausanne, Avenue Pierre-Decker 4, CH-1011 Lausanne, Switzerland.

[3] Wolfson Institute for Biomedical Research and Department of Cell and Developmental Biology, University College London, London WC1E 6BT, United Kingdom.

[4] CNRS UMR 7637, Laboratoire de neurobiologie E.S.P.C.I, 75005 Paris, France.

[5] Department of Genetic and Behavioral Neuroscience, Gunma University Graduate School of Medicine and Japan Science and Technology Agency, CREST, Maebashi 371-8511, Japan.

[6] Department of Adult Psychiatry, University Hospital of Geneva, CH-1211 Geneva 4, Switzerland.

[7] Department of Fundamental Neurosciences, University of Geneva Medical School, CH-1211 Geneva 4, Switzerland.

[8] Geneva Neuroscience Center, University of Geneva Medical School, CH-1211 Geneva 4, Switzerland.

** These authors contributed equally to this work.*

 # Address correspondence to Dr. Cécile Lebrand, EPFL/SV/ISREC/UPBRI, SV 2830, Station 19, CH-1015 Lausanne, Switzerland.

Telephone: +41 21 693 07 85.

Email: cecile.lebrand@epfl.ch

Brief running title:

GABAergic neurons participate in corpus callosum formation and axon guidance.

Abstract (229)

The corpus callosum (CC) plays a crucial role in interhemispheric communication. It has been shown that CC formation relies on the guidepost cells located in the midline region that include glutamatergic and GABAergic neurons as well as glial cells. However, the origin of these guidepost GABAergic neurons and their precise function in callosal axon pathfinding remain to be investigated. Here, we show that two distinct GABAergic neuronal subpopulations converge towards the midline prior to the arrival of callosal axons. Using *in vivo* and *ex vivo* fate mapping we show that CC GABAergic neurons originate in the caudal and medial ganglionic eminences (CGE and MGE) but not in the lateral ganglionic eminence (LGE). Time lapse imaging on organotypic slices and in *vivo* analyses further revealed that CC GABAergic neurons contribute to the normal navigation of callosal axons. The use of *Nkx2.1* knockout (KO) mice confirmed a role of these neurons in the maintenance of proper behavior of callosal axons while growing through the CC. Indeed, using *in vitro* transplantation assays, we demonstrated that both MGE- and CGE-derived GABAergic neurons exert an attractive activity on callosal axons. Furthermore, by combining a sensitive RT-PCR technique with *in situ* hybridization, we demonstrate that CC neurons express multiple short and long range guidance cues. This study strongly suggests that MGE- and CGE-derived interneurons may guide CC axons by multiple guidance mechanisms and signaling pathways.

Keywords

Axonal guidance, cerebral cortex, corpus callosum, GABAergic interneurons, guidance factors

Introduction

The largest commissural tract in the human brain is the corpus callosum (CC) with over 200 million axons that transfer information between the two cerebral hemispheres. Agenesis of the corpus callosum (AgCC) including complete absence, as well as, hypogenesis (partial absence) of the CC is a complex neurodevelopmental disorder. More than 50 different types of CC agenesis have a genetic component and are associated with recognizable syndromes (Paul et al., 2007; Richards et al., 2004). Agenesis of the CC can result from defects during specific steps of callosal development such as cortical neuronal proliferation, specification or migration, as well as axonal guidance through the CC (Paul et al., 2007; Richards et al., 2004). Numerous patients with AgCC exhibit reduced capacity in abstract reasoning, problem solving, generalization and category fluency. Patients with AgCC are also deficient in the comprehension of idioms, proverbs, vocal prosody, and narrative humour (Doherty et al., 2006; Paul et al., 2007) . This may be explained by the fact that the CC is the main path for coordinating syntactic information in the left hemisphere and prosodic information in the right hemisphere. Moreover, structural CC abnormalities have been noticed in some patients with schizophrenia, autism, Tourette's syndrome and attention deficit hyperactivity disorder, even though definitive association with these disorders still remains to be demonstrated (Hallak et al., 2007; Hardan et al., 2000; Paul et al., 2007; Plessen et al., 2006; Seidman et al., 2005).

During development, callosal axons navigate through a complex environment and make several critical decisions before reaching their target (Chedotal, 2010; Kalil et al., 2011; Richards et al., 2004). Growth cones, specialized sensory-motor structures at the leading edge of axons, are able to sense and to interpret different attractive and repellent guidance cues (secreted/diffusible or bound factors) in their environment (Dickson, 2002). The "guidepost" cells are placed at defined and critical positions within the migratory pathway of axons and serve as temporary target points providing the axonal projections with the information required for appropriate guidance (Dickson and Zou, 2010; Jones et al., 2002). The current model proposes that the three midline structures, namely, the glial cells of the glial wedge (GW), the glial sling and the indusium griseum (IG) coordinate midline cortical axon guidance by secreting guidance factors which channel the CC axons into the correct path (Shu et al., 2003a; Shu et al., 2003b; Shu and Richards, 2001; Shu et al., 2003c; Silver et al., 1993; Silver and Ogawa, 1983; Smith et al., 2006). These guidance signalling factors include Netrin1/DCC, Slit2/Robo1, Semaphorin/Neuropilin-1 (Npn-1), ephrins/Eph and Wnt/Ryk (Andrews et al., 2006; Andrews et al., 2007; Bagri et al., 2002; Bush and Soriano, 2009; Fazeli et al., 1997; Gu et al., 2003; Hu et al., 2003; Hutchins et al., 2010; Islam et al., 2009; Keeble et al., 2006; Lopez-Bendito et al., 2007; Mendes et al., 2006; Piper et al., 2009; Ren et al., 2007; Serafini et al., 1996). In addition, observations in mice and humans showed that many neurons are present in the "glial" sling (Jovanov-Milosevic et al., 2010; Ren et al., 2006; Shu et al., 2003a), and scattered neurons were identified in the cat CC during early post-natal life (Riederer et al., 2004; Riederer and Innocenti, 1992). We have previously shown that two transient subpopulations of these neurons, one glutamatergic and one GABAergic, occupy a strategic position in the mouse CC and contribute to the guidance of growing callosal axons (Niquille et al., 2009). In particular, we found that both neuronal populations can attract callosal axons and that this activity is dependent in part on Sema3C function in glutamatergic neurons. Recently, the meninges have also been shown to play a distinct role in the proper formation of the CC by regulating the onset of cortical neurogenesis in embryos (Siegenthaler et al., 2009). It is believed that the

interaction of the meninges, via the secretion of BMP7, with the cingulate neurons, that express Wnt3, regulates CC formation (Choe et al., 2012). BMP7 acts as a negative regulator of callosal axon growth, and the callosal axons overcome this inhibition via the expression of Wnt3 (Choe et al., 2012). Interestingly, BMP7 is also required to control CC midline guidepost cells differentiation (Sanchez-Camacho et al., 2011). Also, Wnt3 expression in the callosal axons is regulated by GDF5 produced by the Cajal-Retzius cells, and GDF5 is further regulated by its inhibitor, Dan produced by the meninges (Choe et al., 2012). In addition, we have showed recently that the regulatory factor RFX3 plays a crucial role during early brain development by indirectly regulating GLI3 activity, which leads to FGF8 upregulation and to disturbed distribution of guidepost neurons that are required for CC morphogenesis (Benadiba et al., 2012). Therefore, these findings raise the possibility that the study of genes controlling CC guidepost cells differentiation or positioning could shed further light on callosal agenesis.

Here, we studied in details the guidepost GABAergic neurons of the CC and showed that they form a heterogeneous population that is generated in the ventral telencephalon and migrates to populate transiently the CC region at the time when callosal axons are approaching the midline. One of these neuronal populations is derived from the MGE, since they are generated from *Lhx6*-expressing precursors. The other population is generated in the CGE as shown by their labelling in 5-HT3a-GFP-expressing transgenic mice. Time-lapse microscopy reveals that GABAergic neurons in CC migrate actively until E14.5 and reduce their mobility from E16.5 to E18.5 as callosal axons crossing the midline make frequent contacts on their surface. Grafting experiments demonstrate that both MGE- and CGE-derived GABAergic neurons exert a direct attractive action on callosal axons. Interestingly, GABAergic neurons of the CC were found to express several guidance factors known to regulate axonal outgrowth, branching formation or cell migration. Moreover, using *Nkx2.1*$^{-/-}$ mice that lack MGE-derived GABAergic interneurons, we confirmed that the guidepost neurons are required for proper navigation of callosal axons across the CC midline.

Together, these results reveal that two distinct classes of transient guidepost GABAergic neurons are important for callosal axon guidance and lay ground for new strategies to characterize the etiology of CC agenesis in humans.

Results

Generation and migration of CC GABAergic neurons prior to callosal axon ingrowth

Our previous work has implicated GABAergic neurons in the formation of the CC (Niquille et al., 2009). In order to further characterize the precise function of the CC GABAergic neurons in the formation of callosal pathways, we analyzed their distribution during development in relation to callosal axons. GABAergic guidepost neurons of the CC were identified using the *GAD67-GFP* mouse line in which green fluorescent protein (GFP) is reliably expressed by GABAergic neurons (Lopez-Bendito et al., 2004; Tamamaki et al., 2003). At E14.5, migrating GAD67-GFP^{+} neurons were properly positioned to guide callosal axons after they leave the cortex overlying the lateral region of the CC (Figure 1A). At E15.5, the callosal axons reach the midline and by E16, the first axons that pioneer the formation of the CC begin to cross the midline and others that are originating from the frontal cortex just start to approach the CC lateral border (Niquille et al., 2009; Ozaki and Wahlsten, 1998; Rash and Richards, 2001). From E15.5 to E18.5, the callosal axons were surrounded by numerous GAD67-GFP positive neurons that have invaded the entire CC white matter (Figure 1B and 1C). From P7 to P14, CC GABAergic neurons disappeared progressively in a spatiotemporal gradient from the medial to the lateral CC regions (Figure 1D and 1E) (Niquille et al., 2009). These results show that during embryonic development transient GABAergic guidepost neurons, positioned at specific locations within the CC, delineate callosal axon paths.

The temporal profile of the embryonic CC GABAergic neuronal production was studied in the embryonic CC with birth-dating experiments. Several studies have mentioned that cortical GABAergic interneurons are mainly generated from the ventral pallium between E12.5 to E16.5 (Anderson et al., 2001; Gelman et al., 2009; Marin and Rubenstein, 2001; Miyoshi et al., 2010; Rubin et al., 2010; Vucurovic et al., 2010). Therefore, 5-bromo2'-deoxy-uridine (BrdU) injections were performed at E12.5, E14.5 and E16.5 in *GAD67-GFP* mouse and brains were processed for BrdU immunostaining when the CC is being formed i.e. at E16.5 and E18.5 (Figure 1F-1J). We found that the GAD67-GFP+ neurons that first reach the CC midline at E16.5 were mainly produced at E12.5 and a very few at E14.5 (Figure 1F-1G and 1K). Similarly also at E18.5, the CC was populated by GAD67-GFP+ GABAergic neurons generated mainly between E12.5 and E14.5 (Figure 1H-1K). GAD67-GFP^{+} neurons generated at E12.5 were found in both the medial and the lateral parts of the E18.5 CC (Figure1H-1K). GAD67-GFP^{+} neurons generated at E14.5 were distributed throughout the entire E18.5 CC, but mainly in the medial parts (Figure 1I-1K). GABAergic interneurons born at E16.5 were rarely observed throughout the CC medial and extreme lateral parts (CC wings, star in Figure 1J1 and Figure 1K). This study indicates that CC GABAergic guidepost neurons are generated principally from E12.5 to E14.5 and migrate into the CC concomitantly to callosal axon ingrowth. Thus, the position and the timing of appearance of these GABAergic interneurons raise the possibility that they might be actively involved in the guidance of callosal axons.

CC guidepost GABAergic neurons originate from the MGE and the CGE

We next characterized the source and molecular identity of these GABAergic neurons that converge to the CC commissure during embryonic development. The embryonic ventral telencephalon, or subpallium, contains distinct progenitor domains, the lateral, medial and caudal eminences (LGE, MGE and CGE) and the preoptic area (Corbin et al.,

2001; Flames et al., 2004; Ghanem et al., 2007; Marin and Rubenstein, 2001). *In vivo* fate mapping studies have revealed that the MGE and the CGE are the primary sites of genesis of a majority cortical interneuron (Butt et al., 2005; Nery et al., 2002; Wichterle et al., 2001). The MGE was believed to be the major contributor in generating cortical GABAergic neurons but the CGE domain has recently been shown to account for 30-40% of them (Miyoshi et al., 2010; Rubin et al., 2010; Rudy et al., 2010; Vitalis and Rossier, 2010; Vucurovic et al., 2010). To determine the precise subpallial origin of CC GABAergic neurons, we have performed fate mapping studies using transplantation experiments, *in vitro* electroporation and genetic lineage tracing (Figures 2 and 3).

First, transplantation experiments in organotypic slices were used to follow the fate of CC GABAergic neurons derived from different subpallial domains. LGE, MGE or CGE explants from E14.5 GAD67-GFP$^+$ mice containing GABAergic precursors, were transplanted into corresponding sites of unlabelled host telencephalic slices including the main body of the CC (Figure 2A and 2B). After one and a half days *in vitro*, LGE-derived GAD67-GFP$^+$ neurons were mostly found within the striatal zone (Figure 2A2). By contrast, numerous MGE- and CGE-derived GAD67-GFP$^+$ neurons were seen to contribute to GABAergic interneurons of the CC using *in vitro* focal electroporation. An expression vector encoding the red fluorescent protein Tomato (*pCAG-IRES-Tomato*) was electroporated either into the LGE (Figure 2B left and 2C), the MGE (Figure 2B right and 2D) or the septum (not shown) of GAD67-GFP$^+$ telencephalic slices. MGE position was ascertained by Nkx2.1 staining (Sussel et al., 1999), which is specifically expressed in this region (Figure 2E). At E14.5, electroporation in the MGE consistently gave rise to GAD67-GFP$^+$ neurons co-labelled in red by Tomato that had migrated into the CC white matter (Figure 2D1-D2). By contrast, electroporation in the LGE or septum (not shown) did not generate GAD67-GFP$^+$/Tomato$^+$ neurons appearing in the CC at any age (Figure 2C).

To further establish the relative contribution of the MGE and CGE domains towards the generation of CC GABAergic guidepost neurons, we performed genetic fate mapping analysis (Figure 3). To selectively fate map MGE-derived postmitotic GABAergic neurons, we crossed *Lhx6-Cre* mice with the reporter line *Rosa26-lox-STOP-lox-YFP* (Fogarty et al., 2007; Srinivas et al., 2001). To visualize LGE/CGE-derived GABAergic neurons, we used a subtractive genetic labelling strategy described previously (Rubin et al., 2010), in which *Dlx1- lox-Venus-Lox* mice referred as *Dlx1-Venus^{fl}* transgenic mice are crossed with *Nkx2.1-Cre* mice. This approach allowed us to visualize GABAergic neurons generated by *Dlx1*-positive subpallial domains except *Nkx2.1*-derived cells. The Venus$^+$ GABAergic neurons have been shown to originate from LGE/CGE domains (Rubin et al., 2010).

We compared the distribution of MGE-derived YFP$^+$ GABAergic neurons in the CC of *Lhx6-Cre/R26R-YFP* embryos with the distribution of LGE/CGE-derived Venus$^+$ neurons in the embryonic CC at E16.5 and at E18.5. While LGE/CGE-derived GABAergic neurons have been shown to be generated and reach the cerebral cortex later than MGE-derived neurons (Anderson et al., 2001; Lavdas et al., 1999; Miyoshi et al., 2010; Rubin et al., 2010; Vucurovic et al., 2010), both populations were present in the CC white matter as early as E16.5 (Figure 3E and 3I). Consistent with previous studies showing that the two neuronal populations initially follow distinct migratory paths (Rubin et al., 2010), MGE-derived YFP$^+$ GABAergic neurons migrated via the MZ, SVZ/IZ and SP routes (Figure 3E) whereas LGE/CGE-derived Venus$^+$ GABAergic neurons travelled exclusively within the SVZ/IZ (Figure 3I). After quantification, MGE

and LGE/CGE were found to generate an equal number of CC GABAergic neurons (YFP^+ neuronal density compare to $Venus^+$ neuronal density at E16.5: $p>0.05$ for medial, lateral and entire CC) (Supplementary Figure S1A). Comparison of the medial and lateral parts of the CC showed that, at E16.5, MGE- and LGE-/CGE-derived GABAergic neurons localized preferentially within the lateral developing CC (neuronal density in the medial CC compared to neuronal density in the lateral CC at E16.5: $p<0.001$ for both neuronal populations) (Figure 3F and 3J, green lines). Two days later at E18.5, both neuronal populations accumulated in abundance within the entire white matter and were distributed homogenously through the medial and lateral CC (neuronal density in the medial CC compare to neuronal density in the lateral CC at E18.5 : $p>0.05$ for both neuronal population) (Figure 3G, 3H, 3K and 3L). At E18.5 in comparison to E16.5, the density of MGE- and of LGE-/CGE-derived neurons significantly increased at the CC midline at the expense of the lateral CC (neuronal density at E16.5 compared to neuronal density at E18.5; $p<0.001$ for both neuronal populations in the medial CC) (Figure 3F compared to 3G and Figure 3J compare to 3K, red lines). The density of the LGE-/CGE-derived $Venus^+$ neuronal population significantly increased throughout the entire CC at E18.5 indicating that CGE-derived neurons most probably continued to migrate to the CC after E16.5 ($Venus^+$ neuronal density at E16.5, Figure 3J compared to $Venus^+$ neuronal density at E18.5, Figure 3K; $p<0.05$ in the entire CC; red lines). The MGE and the LGE/CGE domains provide equal numbers of CC GABAergic neurons in the E18.5 CC (YFP^+ neuronal density compared to $Venus^+$ neuronal density at E18.5: $p>0.05$ for medial, lateral and entire CC) (Supplementary Figure S1B). We furthermore confirmed that all CC GABAergic neurons originated either from the MGE or the LGE/CGE, by comparing the total number of GAD67-GFP^+ CC neurons (Supplementary Figure S1C and S1D) to the sum of YFP^+ neurons and $Venus^+$ neurons in the CC at E16.5 and E18.5. These results show that all the CC GABAergic guidepost neurons originate in the MGE or the LGE/CGE.

To further discriminate between an LGE or a CGE origin, we took advantage of the *5-HTR3a-GFP* mice that express GFP in cortical GABAergic neurons derived specifically from the CGE at embryonic ages (Inta et al., 2008; Lee et al., 2010; Vucurovic et al., 2010). Firstly, we studied the relative distributions of CGE-derived 5-HTR3a-GFP^+ neurons in the CC of E16.5 and E18.5 (Figure 3M, 3N, 3O and 3P). Secondly, we compared the densities of 5-HTR3a-GFP^+ and of $Venus^+$ neurons throughout the CC at the two ages (Supplementary Figure S1A and S1B). Apart from an additional band of 5-HTR3a-GFP^+ neurons present throughout the cortical SP, the CC neuronal distribution was very similar for both neuronal populations indicating that the CGE, in contrast to the LGE, is a major contributor of CC GABAergic interneurons (compare Figure 3M to 4I and Figure 3P to 3L, Supplementary Figure S1A and S1B). Our results therefore show that the guidepost GABAergic neuronal population of the CC is more heterogeneous than previously thought. The CC white matter contains transient GABAergic interneurons that originate equally from two different subpallial domains: the MGE and the CGE.

Guidepost GABAergic neurons help callosal axons outgrowth

To better characterize the dynamic properties and migratory profile of CC GABAergic neurons during embryonic development, we performed confocal time-lapse video microscopy on GAD67-GFP^+ brain slices. From E14.5 to E15.5, we observed that numerous GAD67-GFP^+ neurons exhibited rapid multidirectional movements within the

white matter of the CC (basal rate of migration at E14.5 =25.0 ± 1.0 µm/h, frequency of pauses at E14.5 = 3.5 ± 0.3 pauses/10 hr) (Figure 4A and 4E). In contrast, the majority of CC GAD67-GFP$^+$ neurons exhibited a significant decrease of their basal rate of migration throughout the entire CC at E16.5 (basal rate of migration at E16.5 =14.43 ± 0.68µm/h, E16.5 vs. E14.5 $p<0.001$) and were observed to pause twice as often in this region (frequency of pauses at E16.5 = 7.4 ± 0.3 pauses/10 hrs, E16.5 vs. E14.5 $p<0.001$) (Figure 4B and 4E). At E17.5, CC GABAergic neurons continued to decelerate (basal rate of migration at E17.5 =8.1 ± 0.6 µm/h, E17.5 vs. E16.5, $p<0.001$) while the pausing time reached its maximum value (frequency of pauses at E17.5 = 7.7 ± 0.4 pauses/10 hrs, E17.5 vs. E16.5, $p=0.09$) (Figure 4E). Therefore, while the CC develops, GABAergic neurons have decreased migratory dynamics and pause more often, which is consistent with a guidepost function.

To gain insights into the interactions between CC GABAergic neurons and callosal projections, we analyzed callosal axons navigation in GAD67-GFP$^+$ brain slices. Callosal pioneering axons were visualized with the red fluorescent protein Tomato after *in utero* electroporation at E14.5 or using DiI staining (Figure 5). Using organotypic slices, we were able to examine callosal axons originating from the cingulate and frontal neocortex and growing continuously from the lateral extension of the CC to the midline (Figure 5B1 and 5D1). Interestingly, time lapse sequences revealed that callosal axons grew within the CC by making branch extensions and retractions (Figure 5B2). While growing through the CC neuronal network, the growth cones of callosal axon branches were observed to contact neuritic processes and cell bodies of stationary guidepost GABAergic neurons (Figure 5B2 and 5D2, arrowheads). These cell contacts were better visualized using iso-surface reconstructions that outline the three-dimensional aspects of growth cones and GABAergic cells (Figure 5B3, 5E1 and 5E2). The interactions between callosal axons and CC GABAergic neurons were mostly observed to occur prior to axonal outgrowth (Figure 5B2, t:20'- t:60' and 5D2, t:0'- t:60') and in fewer cases by axonal retraction. The retraction was usually followed subsequently by the formation of new branches (Figure 5B2, t:60'-t:100', empty arrowhead; 5C). Quantifications made on time-lapse movies supported our observations that callosal axons making contacts with CC guidepost GABAergic neurons displayed significantly increased events of axonal outgrowth, as compared to those that did not make contacts (Figure 5C). Our observations thus indicate that transient GABAergic neurons of the CC form a dense cellular network that closely interacts with the growing callosal axons.

In order to study the possible involvement of Nkx2.1-derived GABAergic neurons in guiding axons, we crossed *Nkx2.1*$^{+/-}$ mice (Sussel et al., 1999) with heterozygous *GAD67-GFP* knock-in mice. The sequential crosses allowed us to generate *Nkx2.1*$^{+/+}$*:GAD67-GFP* and *Nkx2.1*$^{-/-}$*:GAD67-GFP* mice which were used to visualize the *GAD67-GFP*$^+$ GABAergic interneurons in wild-type and mutant brains labelled by the GFP antibody. In *Nkx2.1*$^{-/-}$*:GAD67-GFP* embryos, we observed as mentioned previously a loss of Nkx2.1-derived glia (Kessaris et al., 2006; Nery et al., 2001and personal comunication) and a loss of around 60 % of GAD67-GFP$^+$ neurons within the CC (36.8±3.36% of GAD67-GFP$^+$ neurons left in the CC; n=6 sections of *Nkx2.1*$^{+/+}$*:GAD67-GFP* and *Nkx2.1*$^{-/-}$*:GAD67-GFP* mice brains) (not shown). We performed *in utero* electroporation of a *pCAG-IRES-Tomato* plasmid into *Nkx2.1*$^{+/+}$*:GAD67-GFP* and *Nkx2.1*$^{-/-}$*:GAD67-GFP* embryos in order to visualize the callosal axons and GAD67-GFP$^+$ interneurons (Figure 6). This experiment allowed us to detect that the callosal axons were displaying subtle differences between the mutant and

the control. While *Nkx2.1$^{-/-}$:GAD67-GFP* mice exhibited an enlarged CC, the general callosal axon navigation paths seemed to be preserved in the mutant compared to the WT brains. The callosal axons crossed the midline normally and progressed to the contralateral hemisphere. However, high magnification views revealed that the tomato-labelled callosal axons were not properly fasciculated at the midline and displayed aberrant branching patterns (Figure 6B compared to 6A, open arrowheads). The defasciculation of these axons can probably explain the thickening of the CC at the midline. Some of the callosal axons at the midline and post-crossing over of the midline were observed to stray away from the normal path and displayed mistargeting growth trajectories (Figure 6B). These individual misguided axons turned within the tract and astray from the normal trajectory. Confocal time-lapse video microscopy unravelled that growth cones of callosal axons in the *Nkx2.1$^{-/-}$:GAD67-GFP* CC still responded to the remaining GAD67-GFP^{+} GABAergic neurons of the CC and progressed along their normal tracks (Figure 6D compared to 6C) innervating the contralateral hemisphere. However, they formed branched extensions that grew in a disoriented manner compared to the WT axonal branches (Figure 6D compared to 6C). Sometimes, the misrouted axons displayed turning of the primary growth cone at right angles to the normal trajectory (Figure 6D, open arrowheads). The misdirected axons appeared to overlap more often and formed intermingled fascicles, when compared to WT. Some mutant axons displayed repeated retractions exemplified by the quantitative results. Although the WT and *Nkx2.1$^{-/-}$* axons grew at similar speed, many mutant axons were restricted to smaller area when compared to WT (Figure 6D, arrowheads). Thus, the reduced GABAergic neuronal localization in the Nkx2.1$^{-/-}$ mice lead to callosal axon pathfinding defects in the CC tract.

Guidepost GABAergic neurons exert attractive influences on callosal axons

To further understand how CC GABAergic neurons contribute to callosal axon outgrowth, we directly tested whether they could exert an attractive influence on growing axons using grafting experiments in organotypic slices. At E16.5, callosal axons grow through the midline, avoiding the flanking septum and IG which are repulsive for the callosal axons (Figure 7A). In contrast, when explants from the CC of E16.5 GAD67-GFP positive slices (containing GABAergic neurons) were grafted into the non-permissive septal region of the wild-type host slice, numerous DiI-labeled callosal axons were deviated from their normal path and attracted towards the CC explant (Figure 7B). Moreover, we examined whether the CC region comprising GAD67-GFP+ GABAergic neurons exerts an attractive influence on cortical axons by placing E16.5 CC explants, comprising the two neuronal populations of interest, adjacent to explants of the medial cortex (Figure 7F). Indeed, after 2 days *in vitro*, axonal outgrowth in the quadrant closest to the CC aggregate was increased compared to the quadrant furthest away from the aggregate, indicating chemoattraction (Figure 7F2 and 7F4).

We have previously shown that, unlike LGE-derived neurons, MGE-derived GABAergic neurons are able to attract callosal axons. To determine whether CGE-derived GABAergic neurons of the CC have similar attractive properties, we performed heterotopic graft experiments in organotypic slices. To directly test the roles of these two populations of CC GABAergic neurons, we grafted in the septum of E16.5 host slices, explants coming from E16.5 GAD67-GFP^{+} MGE or CGE which both generate the GABAergic neurons of the CC (Figure 7D and 7E, respectively). Interestingly, numerous axons left the callosal track, penetrated the repulsive septum and grew in between

migrating GAD67-GFP$^+$ neurons originating from the MGE transplant (Figure 7D, arrowheads, n=14/19) or from the CGE transplant (Figure 7E, arrowheads, n=11/13). MGE-derived and CGE-derived neurons attracted equally callosal axons. This attraction was specific for MGE-derived and CGE-derived neurons, since LGE control explants did not attract callosal axons (Figure 7C; n= 10/12). These observations indicate that CGE-derived GABAergic neurons directly contribute, in addition to MGE-derived neurons, to an attractive activity on callosal axons.

CC GABAergic neurons express several guidance factors and cell adhesion molecules

To characterize the molecular mechanisms underlying the guidance effects of CC GABAergic guidepost neurons on callosal axons, we investigated whether GABAergic neurons express short- or long-range guidance factors (Figure 8). First, we studied the gene expression profile at E16.5 of GAD68-GFP+ neurons in CC and the adjacent cortex using a highly sensitive RT-PCR method (Rufer et al., 2005; Speiser et al., 2006) (Figure 8A1). After micro-dissection and cell dissociation, 300 GFP+ and 300 GFP- cells of the CC and adjacent cortex were directly isolated by FACS sorting and screened for various guidance factors using RT-PCR together with subsequent amplification with global and specific primers (Figure 8A1-A2). We examined the expression profile of the CC neurons for guidance cues that are known to regulate outgrowth, branching or pathfinding in the CC and in other axonal tracts during development (Figure 8A3). These include: (1) trophic factors (NGF, BDNF, FGF), (2) secreted guidance factors (Netrins, Slits, Semaphorins, ephrins) and their receptors (Ephs and Npns), as well as (3) cell adhesion molecules from the L1 family of CAMs (L1, NrCAM, NCAM, Ncadh) and from the TAG1/axonin-1 family of GPI-linked CAMs (TAG1) (Chedotal, 2010; Dickson, 2002; Egea and Klein, 2007; Mann et al., 2007; Stoeckli and Landmesser, 1998; Suter and Forscher, 2000; Wilkinson, 2001; Yazdani and Terman, 2006; Yu and Bargmann, 2001). We found that GAD67-GFP+ neurons did not express Netrins, Slits, or the trophic factors (Figure 8A3, + bands). In contrast, they did express *Sema3A* and Neuropilin receptors (*Npn1 and Npn2*), several ephrins (*ephrinB1, ephrinB2, ephrinA1, ephrinA4*) and Eph receptors (*EphB2, EphB3, EphA4*), as well as cell adhesion molecules from the L1 family (*NrCAM, L1, NCAM1, Ncadh*) (Figure 8A3, + bands). To confirm that CC GABAergic neurons specifically expressed these factors, we performed *in situ* hybridization or immunostaining. In accordance with the RT-PCR results, we never detected expression of *Netrins, Slits, ephrinA3, ephrinB3, EphB1* nor *TAG1* in the CC GAD67-GFP+ neurons (not shown and Figure 8A3). *NrCAM, ephrinA1, ephrinA4, and ephrinA5* were only observed at low levels within the cerebral cortex at E16.5 (not shown). *Npn-1* while strongly expressed by CC white matter cells was only detected sporadically in a few GABAergic neurons (not shown). Interestingly, we found that *Sema3A,* Npn-2 and numerous ephrins and Eph receptors (*ephrinB1, ephrinB2, EphA4 and EphB2*) were expressed at high levels by GAD67-GFP+ neurons of the CC at E16.5 (Figure 8B-8G, arrowheads). The guidance factors were not uniformly expressed by all CC GABAergic neurons (open arrowheads) indicating that these neurons have distinct guidance properties. The factors were also detected in the GFP- pool of CC cells comprising other neurons, glia or precursors (Figure 8A3, - bands; Figure 8B2-8G2, *). In accordance with our previous study (Niquille et al., 2009) and our RT-PCR results the *Sema3C* was only found within the glutamatergic neurons and not the GABAergic neurons of the CC (Figure 8A3 and not shown).

Taken together, our time-lapse and transplantation experiments indicate that CC neurons exert short- and long-range attractive influences on callosal axons, which are mediated by both MGE- and CGE-derived GABAergic neurons. In search for candidate molecular signals, we found that CC GABAergic neurons express different combinations of secreted guidance factors and cell adhesion molecules that possibly participate to their guidepost function for callosal axons.

Discussion

Our study reveals that GABAergic neurons are important for regulating axonal guidance in the embryonic CC. We identified two distinct GABAergic neuronal subpopulations, one originating from the MGE and the other from the CGE, which transiently occupy the developing CC. These two neuronal populations exhibit a reduced motility after they have reached the midline and occupy a strategic position for guiding ingrowing callosal axons. Callosal axons while navigating through the CC are seen to make close contacts with the stationary GABAergic neurons. Interestingly, both MGE and CGE GABAergic neuronal populations exert an attractive activity on callosal axons. In search for candidate molecular signals mediating the attractive activity on callosal axons, we found that CC GABAergic neurons express several types of guidance factors and cell adhesion molecules. By revealing a role for GABAergic neurons in the pathfinding of callosal axons, our study brings new understanding about neuronal development and new perspectives on pathophysiological mechanisms altering CC formation in humans.

GABAergic neurons act as guidepost cells in the CC

During development, callosal axons make multiple guidance choices to cross the midline and reach their contralateral cortical targets (Chedotal, 2010; Richards et al., 2004). Our previous study revealed that, in addition to the characterized role of glial cells, transient glutamatergic and GABAergic neurons are essential for the control of axon guidance in the developing CC (Niquille et al., 2009). Here, we have specified the origins and functions of the GABAergic neurons of the CC. We have discovered that CC GABAergic neurons arise from two distinct sources, follow different migratory routes and converge to the CC midline before the arrival of callosal axons. Our *in vitro* and genetic fate-mapping experiments indicate that the GABAergic neurons of the CC originate equally from the MGE and the CGE. Similarly, the MGE and the CGE have been shown to provide cortical GABAergic interneurons (Anderson et al., 1997; Anderson et al., 2002; Butt et al., 2005; Fogarty et al., 2007; Lee et al., 2010; Marin and Rubenstein, 2001; Marin and Rubenstein, 2003; Metin et al., 2006; Miyoshi et al., 2010; Nery et al., 2002; Rubin et al., 2010; Rudy et al., 2010; Vitalis and Rossier, 2010; Vucurovic et al., 2010; Wichterle et al., 2001; Xu et al., 2004). In addition, grafting experiments indicate that while originating from different sources, both MGE and CGE GABAergic migrating neurons possess the same capacity to chemoattract callosal axons. Interestingly, the different migration paths and distributions of MGE- and CGE-derived GABAergic neurons through the CC at E16.5 may allow these guidepost neurons to play complementary attractive effects on growing callosal axons.

Time lapse analysis allowed us to specify the nature of the cellular interactions between callosal axons and CC GABAergic neurons. In accordance with a previous study made in living CC slices from neonatal hamster (Halloran and Kalil, 1994), we observed that callosal axons exhibit a complex behaviour characterized by the extension of new branches that are either stabilized or retracted. Interestingly, our work indicates that this complex growth cone behaviour could be related to growth cone interactions with CC guidepost GABAergic neurons. Cell contacts with CC GABAergic neurons were observed more often to be accompanied by new branch formation and increased axonal outgrowth and in fewer cases to correlate with growth cone collapse and branch retraction. The presence of these GABAergic neurons is required for the proper navigation of callosal axons, since the reduction of MGE-derived GABAergic interneurons in the CC of *Nkx2.1*$^{-/-}$ caused branching and outgrowth abnormalities of

callosal axons. However, the observed phenotype in *Nkx2.1*$^{-/-}$ is less drastic than the patterning defects seen in Mash1 mutants described by our group previously (Niquille et al., 2009). The differences can be attributed to the fact that Mash1 mutant embryos are nearly devoid of the GABAergic neurons that originate from the ventral telencephalon (Niquille et al., 2009) whereas the Nkx2.1$^{-/-}$ embryos loose about 60% of the MGE-derived GABAergic neurons only. These results, thus, unravel that these neurons are important for the correct behavior of callosal axons. Altogether, time-lapse and transplantation experiments indicate that CC GABAergic neurons exert attraction on callosal axons.

This function of CC CGE and MGE-derived GABAergic neurons as guidepost cells fits in nicely with the finding that thalamo-cortical axon growth depends instead on the ventral migration of LGE-derived GABAergic neurons within the ventral telencephalon (Lopez-Bendito et al., 2006). These studies altogether point out the high degree of specificity of each type of guidepost GABAergic neuronal population that are involved in the development of different axonal paths (cortico-cortical versus thalamo-cortical). Therefore, transient CC guidepost GABAergic neurons constitute a remarkable mechanism that allows the timely arrangement of guidance cues required for callosal axons pathway formation.

Cellular and molecular mechanisms of callosal axon guidance

To further understand the molecular mechanisms underlying the guidance effects of CC GABAergic guidepost neurons on callosal axons, we investigated in detail their expression profile for guidance factors. Our results indicate that CC GABAergic neurons expressed the Sema3A and Npn-2 receptors, several ephrins (B1/B2) and Eph (B2/B3/A4) receptors, as well as cell adhesion molecules (Ncadh, Ncam1) that help to direct axonal outgrowth. In our study, the guidance factors were not uniformly expressed by all CC GABAergic neurons indicating that these neurons form heterogeneous populations concerning their guidance properties. It will be interesting in the future to define whether this heterogeneity is linked to differences of their origin sites (MGE versus CGE) and whether they have different but complementary roles to play during guidance. This screen nicely complements a previous study showing that the expression of cell surface genes such as Ncam1, Sema3a but not Npn-1 is enriched in E15.5 cortical migrating interneurons (Batista-Brito et al., 2008).

These results are in perfect accordance with previous reports about the expression of several of these guidance factors (ephrins/Eph and semaphorins/Neuropilins) in the CC and surrounding regions (glial wedge, indusium griseum, septum) during development (Bush and Soriano, 2009; Gu et al., 2003; Hatanaka et al., 2009; Mendes et al., 2006; Niquille et al., 2009; Piper et al., 2009; Zhao et al., 2011). Their related receptors (ephrins/Eph and neuropilin-1) are found to be expressed by callosal axons through E15 to E17, the period at which pioneer callosal axons cross and extend to the contralateral hemisphere. Finally, these numerous guidance factors and their cognate receptors have been implicated in orienting the CC axons at critical choice points.

Previous studies on CC formation highlighted the role of glial cells in guiding callosal axons and proposed that most of these guidance cues are expressed by guidepost glial cells of the CC (Bush and Soriano, 2009; Gu et al., 2003; Islam et al., 2009; Keeble et al., 2006; Mendes et al., 2006; Piper et al., 2009; Shu and Richards, 2001; Shu et al., 2003c). Indeed, studies have nicely demonstrated that the guidepost glia of the glial wedge and indusium griseum direct callosal pathfinding at the midline by secreting

guidance factors Wnt5a and Slit2 (Keeble et al., 2006; Shu and Richards, 2001; Shu et al., 2003c). Additional works have shown that for EphB1/B2/B3/A4 located on callosal axons, the potential binding partners, ephrins B1/B2/B3 are expressed by strategic midline guidepost glia and may use forward signal to guide axons (Mendes et al., 2006). Interestingly, ephrin B1 and B2 present on callosal axons will act by reverse signaling after binding EphB2 expressed by the glial cells of the glial wedge and indusium griseum (Bush and Soriano, 2009; Mendes et al., 2006).

However, we previously demonstrated that guidepost glutamatergic neurons of the CC have an attractive activity on callosal axon navigation, partly via Sema3C-Npn1 signaling (Niquille et al., 2009). In addition, we show here that CC axonal guidance requires the additional presence of two other GABAergic neuronal subpopulations. Our screen on guidance molecules clearly indicates that the CC GABAergic neurons express different combinations of guidance molecules or receptors such as Sema3A, ephrinB1 and EphB2 that have been already shown to be involved in CC development (Bush and Soriano, 2009; Mendes et al., 2006; Zhao et al., 2011). Based on these expression profiles and our results, one can hypothesize that during development multiple interactions may take place between the ephrins and their respective Eph receptors either between callosal axons and guidepost glia, and/or between callosal axons and guidepost neurons. In addition, CC guidepost glutamatergic neurons by expressing the Sema3C, and GABAergic neurons by expressing the Sema3A may collaborate in guiding Npn-1 callosal axons. While the Sema3A may act globally as a repulsive signal on cortical axons (Bagnard et al., 1998; Zhao et al., 2011), this repulsive activity may be converted to attraction when the Npn-1 receptor forms transmembrane interaction with L1 or depending on the cyclic nucleotide cAMP/cGMP ratios (Bashaw and Klein, 2010; Castellani et al., 2002). Neuropilin receptors require a signaling co-receptor to mediate semaphorin function (Mann et al., 2007; Yazdani and Terman, 2006). The transducers and signaling pathway that mediate Npn-1 responses on callosal axon guidance remain so far to be defined. Furthermore, the guidance cues expressed by CC GABAergic neurons (ex: Sema3A) may play a role not only in axonal guidance but also in other functions such as cell migration, dendrite and branch formation, as well as synaptogenesis (Bagri and Tessier-Lavigne, 2002; Bashaw and Klein, 2010; Chen et al., 2008; Mann et al., 2007; Marin et al., 2010; Polleux et al., 2000).

Conclusion

As a model, we propose that the CC formation requires the presence of guidepost glial cells as well as specific guidepost neuronal populations. Glia and neurons by secreting short and long range distance guidance cues cooperate to guide callosal projections. Therefore, the relative contribution of individual neuronal or glial populations in the guidance of callosal axons remains largely to be investigated to understand CC guidance mechanisms. Specific inactivation of genes for guidance factors in guidepost neurons or glia and specific cell ablation strategies will probably allow us in the future to get a better picture of the involved underlying mechanisms.

Materials and Methods

Animals

All studies on mice of either sex have been performed according to the national and international guidelines and with the approval of the Federation of Swiss cantonal Veterinary Officers (2164). Wild-type mice maintained in a C57Bl/6 genetic background were used for developmental analysis of the CC. We used heterozygous *GAD67⁻GFP* knock-in mice, described in this work as *GAD67-GFP* mice (Tamamaki et al., 2003). GAD67⁻GFP embryos could be recognized by their GFP fluorescence. NINDS GENSAT BAC transgenic mice for *5-HT$_{3a}$-EGFP* (MMRC) referred here as *5-HT$_{3a}$-EGFP* were maintained in a C57Bl/6 background and were recognized by their GFP fluorescence (Heintz, 2001). We used wild-type (+/+), heterozygous (+/-) and homozygous mutant (-/-) *Nkx2.1* mice (Flames et al., 2007; Kimura et al., 1996; Sussel et al., 1999), which are referred as *Nkx2.1$^{+/+}$*, *Nkx2.1$^{+/-}$* and *Nkx2.1$^{-/-}$* in this work. PCR genotyping of these lines was performed as described previously (Lopez-Bendito et al., 2006). Heterozygous embryos did not show any phenotype and were used as controls. The *Nkx2.1-Cre*, *Lhx6-Cre* and *Dlx1-lox-Venus-lox* transgenic mice have been described previously (Fogarty et al., 2007; Kessaris et al., 2006; Rubin et al., 2010). The reporter mouse *Rosa26R–Yellow fluorescent protein (YFP*) (Srinivas et al., 2001) was used to reliably express YFP under the control of the Rosa26 promoter upon Cre-mediated recombination. Embryos were recognized by their YFP fluorescence.

In utero electroporation

To perform *in utero* electroporation, we adapted our protocol from the one described previously (Cancedda et al., 2007). E14.5 timed-pregnant *GAD67-GFP* mice were anesthetized with isoflurane (3.5% during induction and 2.5% during surgery) and embryos were exposed within the intact uterine wall after sectioning the abdominal wall. The DNA solution containing the expression vector encoding the red fluorescent protein (*pCAG-IRES-Tomato*) (2 mg/ml) together with the dye Fast Green (0.3 mg/ml; Sigma, St. Louis, MO) was pressure injected focally (1–2 µl) into the lateral ventricle of embryos through a glass micropipette using a PicoSpritzer III (Parker Hannifin, Cleveland, OH). Each embryo, while still being within the uterus, was placed between tweezer-type electrodes (System CUY-650P5 Nepa Gene Co, Chiba, Japan) and was electroporated with five electrical square unipolar pulses (amplitude: 45 V; duration: 50 ms; intervals: 950 ms) powered by a BTX electroporator apparatus (model BTX ECM 830; Harvard Apparatus, Holliston, MA). By orienting the tweezer-type electrodes, we were able to preferentially electroporate dorsal pallium precursors that give rise in part to pyramidal callosally-projecting neurons (Borrell et al., 2005). The embryos were quickly placed back into the abdominal cavity and the muscular and skin body wall layers were sutured. The embryos were allowed to develop until E16.5.

Slice cultures

For E14.5 to E16.5 CC slice cultures, we used an *in vitro* model of CC organotypic slices that has been previously described (Niquille et al., 2009). Embryos were dissected in ice cold dissecting medium (MEM Gibco ref 11012-044 with 15 mM glucose and 10 mM Tris pH7-9). Brains were isolated and embedded in 3% low-melting point agarose (Invitrogen). 250 µm thick coronal sections were made using a vibratome and slices at

the level of the CC were collected in cold dissecting medium. CC slices were cultured on nucleopore Track-Etch membrane (1 μm pore size; Whatman) or millicell inserts (0.4 μm pore size; Millipore) in slice culture medium (SCM) (BME/HBSS (Invitrogen) supplemented with 1% glutamine, 5% horse serum, and Pen/Strep (Lopez-Bendito et al., 2006).

Transplantation experiments

To define the origin of CC GABAergic neurons, we performed transplantation experiments of LGE, MGE and CGE ventral regions known to generate cortical GABAergic neurons. For transplantation experiments, slices from E14.5 and E16.5 GAD67-GFP$^+$ embryos were selected and small explants comprising the ventricular (VZ) and subventricular (SVZ) proliferating zones of the LGE, MGE and CGE were manually excised using tungsten needles and transplanted into the corresponding zones of GAD67-GFP$^-$ host slices.

To determine the possible function of LGE-, MGE- and CGE-derived CC GABAergic neurons in attracting callosal axons, we transplanted small explants of E16.5 GAD67-GFP$^+$ LGE, MGE or CGE into the septum of E16.5 GAD67-GFP$^-$ host slices. The study of early callosal axon navigation was performed after insertion of small crystals of 1,1'-dioctadecyl 3,3,3',3'-tetramethylindocarbocyanine perchlorate (DiI) into the frontal cortex to label cortical axons. After 36-72 hours, the slice cultures were fixed and we analysed neuronal migration or callosal axon trajectories by using confocal microscopy. In this assay, cases with axons growing along GAD67-GFP+ neurons originating from the MGE or CGE transplants were counted as positive results for attraction.

***In vitro* focal electroporation**

We applied an *in vitro* focal electroporation method using a Nepagene apparatus to transfect an expression vector into telencephalic slices (Stuhmer et al., 2002). E14.5-E16.5 organotypic coronal slices from *WT* or *GAD67-EGFP* embryos were obtained as described above. The expression vectors encoding the green (*pCAG-IRES-EGFP)* or the red (*pCAG-IRES-Tomato*) fluorescent proteins were electroporated at a concentration of 1mg/ml in sterile PBS 1X (Sigma, St. Louis, MO). Expression vectors were focally injected through a glass micropipette into the LGE or the MGE using a PicoSpritzer III (Parker Hannifin, Cleveland, OH) and the slices were electroporated between platinum Petri-dish and cover square platinum electrodes (System CUY-700-1 and CUY-700-2; Nepa Gene Co, Chiba, Japan) with two unipolar square pulses (amplitude: 100 V; duration: 5 ms; intervals: 500 ms) generated by a CUY21EDIT Electroporator (Nepa Gene Co, Chiba, Japan).

Confocal Time-Lapse Microscopy

For imaging neurons, slices were cultured on nucleopore Track-Etch membranes (1 μm pore size; Whatman) in tissue dishes containing 3ml of SCM medium (BME/HBSS supplemented with glutamine, 5% horse serum and Pen/Strep). CC GABAergic interneuron migration paths and dynamics were studied in coronal CC slices of GAD67-GFP transgenic mice from E14.5 to E18.5. To visualize callosal axons, the plasmid encoding the red fluorescent protein (*pCAG-IRES-Tomato)* was electroporated *in utero* into the dorsal pallium progenitors of E14.5 embryos that generate callosally projecting

neurons. In some additional experiments, small dye crystals were implanted within the frontal cortex of GAD67-GFP sections made from E16.5 to E18.5. We imaged growth cone dynamics and outgrowth properties of frontal callosal axons that were found to grow continuously from the lateral extension of the CC to the midline after E16.5. After 15-20 hrs in culture, slices were placed in an open perfusion chamber on the stage of an upright Leica SP5 confocal microscope. Temperature was maintained at 37ºC with the aid of a microscope incubator system (Life Scientific, Switzerland) and slices were perfused with SCM medium containing a gas mixture of 5% CO2/ 95% O2. GAD67-GFP positive CC neurons and callosal axons labelled with Tomato were imaged with a 20X, a 40X, or a 60X immersion lens at 15 or 20 minute intervals using the fast scan function of the Leica SP5 confocal microscope resonant scanner. Image captures and all peripherals were controlled with Leica software. Pictures were processed and converted into *.AVI movies using Imaris and Metamorph 6.0. Migration parameters (basal rate of migration, frequency and duration of the intervening pauses) were determined by measuring movements every 15-20 minutes during 5 hours while the neurons were migrating through the CC white matter. Using the tracking function of Metamorph software 6.0, a total of 70 GAD67-GFP neuron traces were analyzed at E14.5 and at E16.5; and 35 traces at E17.5.

Immunocytochemistry

Embryos were collected after caesarean section and quickly killed by decapitation. Their brains were dissected out and fixed by immersion overnight in a solution of 4% paraformaldehyde in 0.1 M phosphate buffer (pH 7.4) at 4°C. Postnatal mice were profoundly anaesthetized and perfused with the same fixative, and their brains post-fixed for 4 hours. Brains were cryoprotected in a solution of 30% sucrose in 0.1 M phosphate buffer (pH 7.4), frozen and cut in 50 µm-thick coronal sections for immunostaining.

Mouse monoclonal antibody was: BrdU (Monosan, Am. Uden, Netherlands). Rat monoclonal antibodies were: L1 (Chemicon, Temecula, CA) and SNAP25 (Stemberger Monoclonal Inc., BA). Rabbit polyclonal antibodies were: Calbindin (Swant, Bellinzona, Switzerland); Calretinin (Swant, Bellinzona, Switzerland); GFAP (DAKO, Carpinteria, CA); GFP (Molecular Probes, Eugene, OR); Nkx2.1 (Biopat, Caserta, Italy); GABA (Sigma, St Louis, MO) and NPY (Sigma, St Louis, MO). Goat polyclonal antibodies were: Calretinin (Swant, Bellinzona, Switzerland) and Npn-1 (R&D System, Minneapolis, MN).

Fluorescence immunostaining was performed as follows: unspecific bindings were blocked during preincubation and incubations after adding 2% normal horse serum in PBS 1X solution with 0.3% Triton X-100. The primary antibodies were detected with Cy3-conjugated (Jackson ImmunoResearch laboratories, West Grove, PA) and Alexa488-, Alexa594- or Alexa647-conjugated antibodies (Molecular Probes, Eugene, OR). Sections were counterstained with Hoechst 33258 (Molecular Probes), mounted on glass slides and covered in Mowiol 4-88 (Calbiochem, Bad Soden, Germany).

DAB immunostaining was performed as follows: Endogenous peroxidase reaction was quenched with 0.5% hydrogen peroxide in methanol, and unspecific binding was blocked by adding 2% normal horse serum during preincubation and incubations in the Tris-buffered solutions containing 0.3% Triton X-100. The primary antibodies were detected with biotinylated secondary antibodies (Jackson ImmunoResearch, West Grove, PA) and the Vector-Elite ABC kit (Vector Laboratories, Burlingame, CA). The slices were mounted on glass slides, dried, dehydrated, and covered with Eukitt.

Axonal tracing

After overnight fixation in 4% PFA at 4°C, fine glass needles covered with the fluorescent carbocyanide dye DiI (1,1'-dioctadecyl 3,3,3',3'-tetramethylindocarbocyanine perchlorate or DiA (4-[4-(dihexadecyl amino)styryl]*N*-methyl-pyridinium iodide (Molecular Probes) were placed in single or multiple locations in the neocortex (Metin and Godement, 1996). After 4-8 weeks at 37^{o}C in 4% PFA to allow dye diffusion, the sample were embedded in 5% agarose and cut into 100 µm thick sections on a vibratome. Counterstaining was performed using Hoechst (Molecular Probes).

Single RT-PCR

After microdissection, GABAergic neurons of the CC and of the bordering cortical area, labelled for GAD67-GFP, are isolated by FACS sorting and mRNAs for guidance cues are screened by sensitive RT-PCR (Rufer et al., 2005). The cDNA amplification and screen is performed in 6 steps: (1) the 300 GFP+ and 300 GFP- cells are isolated by FACS sorting, (2) the lysis of the sorted cells and the reverse transcription of total mRNA into cDNA are performed simultaneously, (3) the cDNA is precipitated, (4) the homopolymeric 3'-oligo(dA) tailing is done on precipitated cDNA, (5) the cDNAs are globally amplified by PCR with the aid of oligo-dT Iscove primers, and (6) the genes for guidance cues are screened by PCR using specific primers. GAD67-GFP+ neurons (labelled as R2) corresponding to 11.5% of the total CC cells population are purified by flow cytometry. The expression profile of the flow-cytometer sorted GFP+ and GFP- cell fractions ascertained with specific primers against the various cell makers and guidance cues of interest. Using primers for GAD67, we can verify the selectivity of the FACS sorting method since GFP+ neurons but not GFP- cells express GAD67. Using selective primers for guidance cues, GFP+ and GFP- CC cells were screened for: (1) trophic factors (NGF, BDNF, FGF), (2) secreted guidance factors (Netrins, Slits, Semaphorins, ephrins) and their receptors (Ephs and Npns), as well as (3) cell adhesion molecules from the L1 family of CAMs (L1, NrCAM, NCAM, Ncadh) and from the TAG1/axonin-1 family of GPI-linked CAMs (TAG1).

***In situ* hybridization**

Sema 3A plasmid was linearized with Not1 (New England Biolabs) for antisense RNA synthesis by T3 polymerase (Promega). Sema3C plasmid was linearized with EcoRI (New England Biolabs) for antisense RNA synthesis by T7 polymerase (Promega) and with XhoI (New England Biolabs) for sense RNA synthesis by T3 polymerase (Promega). TAG-1 plasmid was linearized with XbaI (New England Biolabs) for antisense RNA synthesis by T3 polymerase (Promega) and with HindIII (New England Biolabs) for sense RNA synthesis by T7 polymerase (Promega). NrCAM plasmid was linearized with EcoRI (New England Biolabs) for antisense RNA synthesis by T7 polymerase (Promega). EphA4, Npn-1, EphB1 plasmids were linearized with SacI (New England Biolabs) for antisense RNA synthesis by T3 polymerase (Promega). ephrinB2 and ephrinA3 plasmid were linearized with BamH1 (New England Biolabs) for antisense RNA synthesis by Sp6 polymerase (Promega). ephrinB3 plasmid was linearized with HindIII (New England Biolabs) for anti-sense RNA synthesis by T7 polymerase (Promega). ephrinA1 plasmid, EphA3 and EphA5 were linearized with Kpn1 (New England Biolabs) for antisense RNA synthesis by T7 polymerase (Promega). ephrinA4

plasmid and EphB3 were linearized with SacII (New England Biolabs) for antisense RNA synthesis by T3 polymerase (Promega). ephrinA5 plasmid was linearized with BamH1 (New England Biolabs) for antisense RNA synthesis by T7 polymerase (Promega).Slit2 plasmid was linearized with Xba1 (New England Biolabs) for antisense RNA synthesis by T7 polymerase (Promega). For *in situ* hybridization, brains were dissected and fixed by immersion overnight at 4°C in a solution containing 4% paraformaldehyde (PFA) in PBS. 100 µm free-floating vibratome sections were hybridized with digoxigenin-labeled cRNA probe as described before (Garel et al., 1997). To combine *in situ* hybridization and immunofluorescence, Fast Red (Roche) was used as an alkaline phosphatase fluorescent substrate.

Imaging

DAB stained sections were imaged with a Zeiss© Axioplan2 microscope equipped with 10×, 20× or 40× Plan-NEOFLUAR objectives and coupled to a CCD camera (Axiocam MRc 1388x1040 pixels). Fluorescent-immunostained sections were imaged using confocal microscopes (Zeiss LSM 510 Meta, Leica SP5 or Zeiss Qasar 710) equipped with 10×, 20×, 40×oil Plan-NEOFLUAR and 63×oil, 100×oil Plan-Apochromat objectives. Fluorophore excitation and scanning were done with an Argon laser 458, 488, 514 nm (blue excitation for GFP and Alexa488), with a HeNe laser 543 nm (green excitation for Alexa 594, CY3 and DiI), with a HeNe laser 633 nm (excitation for Alexa 647 and CY5) and a Diode laser 405 nm (for Hoechst-stained sections). Z-stacks of 10-15 planes were acquired for each CC coronal section in a multitrack mode avoiding crosstalk. Z-stacks of 40-50 sections were acquired for each CC section for the creation of isosurfaces with Imaris 6.0 software (Bitplane Inc.).

All 3D Z stack reconstructions and image processings were performed with Imaris 6.0 software. To create real 3D data sets we used the mode “Surpass”. The generation of iso-surfaces (object defining a surface surrounding voxels located between two threshold values) allowed us to visualize the contours of cells and of growth cones. The colocalization between two fluorochromes was calculated and visualized by creating a yellow channel. Figures were processed in Adobe Photoshop CS2 and schematic illustrations were produced using Adobe Illustrator CS2.

CC GABAergic neuronal population analysis

In 50 µm CC sections of *Lhx6-Cre/R26R-YFP, Nkx2.1-Cre/Dlx1-Venus*^{fl}, *GAD67-GFP* and *5-HTR3a-GFP* embryos, GABAergic neurons of the CC were counted at E16.5 and E18.5 as the number of cells labelled respectively for the YFP, Venus or GFP from at least 5 sections per condition. To study the density of GABAergic neurons through the CC, the values were quantified on 4 planes of the CC section stacks and were reported per surface unit (number of cells/mm^2). The cell densities were determined in two CC areas (midline and lateral) and in the entire CC area (total). Based on our work, we considered that the CC is divided into two regions: medial and lateral. The medial part is bordered dorsally by the IG and the longitudinal fissure and ventrally by the glial wedge and the dorsal limit of the septum. The lateral part comprises the white matter bordered by the cingulate cortex dorsally, and by the ventricular zone between the glial wedge and the medio-dorsal angle of the lateral ventricle towards the ventricular side.

Ultrastructure

The E16.5 and E18.5 embryos were killed by decapitation. Brains were dissected and fixed by immersion for 24 hours at 4°C in a solution containing 2% glutaraldehyde and 4% paraformaldehyde in 0.1 M phosphate buffer (pH 7.4) with 2% sucrose. The brains were then rinsed in 0.1 M cacodylate buffer (pH 7.4), post-fixed at room temperature for 2 hours in 1% OsO_4, dehydrated in series of graded ethanol and embedded in Epon. The regions containing the CC of the embedded brains were trimmed and mounted on blocks to cut semi-thin and ultra-thin sections. The ultrathin sections were mounted on formvar-coated single slot grids and contrasted with 2% uranyl acetate and 0.2% lead citrate.
For preembedding immunocytochemistry, embryonic brains were fixed by immersion in a solution containing 4% paraformaldehyde and 0.1% glutaraldehyde in 0.1M phosphate buffer (pH=7.4) supplemented with 2% sucrose for 24 hours. Fifty micron-thick sections cut with a Vibratome were immunoreacted with the same protocol as for light microscopy DAB staining, except that the detergent was omitted in all the solutions. Following the DAB reaction, sections were dehydrated and embedded in Epon. The plastic embedded specimens containing a DAB reacted section were prepared for ultra-thin sectioning following the same protocol as above.

Statistical analysis

For all analysis, values from at least three independent experiments were first tested for normality. Values that followed a normal distribution were compared using Student's *t*-test. Values that did not follow a normal distribution were compared using Mann-Whitney and Kolmogorov-Smirnov non-parametric tests.

Atlas and nomenclature

The nomenclature for callosal development is based on the “Atlas of the prenatal mouse brain” (Uta B. Schambra, Jean M. Lauder, and Jerry Silver, Academic Press Inc., 1992).

Abbreviations list

5-HTR3a	Serotonin receptor 3a
5-HTR3a-GFP	Bacterial artificial chromosome (Rufer et al.) 5-HT3a GFP transgenic mouse
BrdU	5-bromo2'-deoxy-uridine
CB	Calbindin
CC	Corpus callosum
CCi	Cingulate cortex
CFr	Frontal cortex
CGE	Caudal ganglionic eminence
CPa	Parietal cortex
CP	Cortical plate
CPN	Callosal projection neurons
CR	Calretinin
CSB	Corticoseptal boundary
DCC	Deleted in colorectal cancer
Dlx1	Distal-less homeobox gene 1
Dlx1-Venus^{fl}	Mouse with lox-Venus-lox construct under control of the *Dlx1* promoter
DiI	1,1'-dioctadecyl 3,3,3',3'-tetramethylindocarbocyanine perchlorate
Eph	Ephrin receptor
GABAergic	γ aminobutyric acidergic
GAD65/67	Glutamate decarboxylase 65/67
GAD67-GFP	GAD67-GFP knock-in mouse
GFAP	Glial fibrillary acidic protein
GFP	Green fluorescent protein
GW	Glial wedge
HIC	Hippocampal commissure
IG	Induseum griseum
IZ	Intermediate zone
KO	Knockout
L1	L1CAM cell adhesion protein
LGE	Lateral ganglionic eminence
Lhx6	LIM homeobox gene 6
Lhx6-Cre	Mouse with the Cre recombinase under control of the *Lhx6* promoter
Mash1	*Ascl*, Mammalian achaete-scute homolog
MGE	Medial ganglionic eminence
MZ	Marginal zone
Nkx2.1	Thyroid transcription factor gene 1 (TTF-1)
Nkx2.1-Cre	Mouse with the Cre recombinase under control of the *Nkx2.1* promoter
Npn-1	Neuropilin1
NPY	Neuropeptide Y
PB	Probst bundle
PFP	Perforating fibre pathway
PP	Preplate

R26R-YFP	Rosa26-lox-STOP-lox-YFP reporter mouse
Robo1	Roundabout homolog 1
Ryk	Wnt tyrosine-kinase receptor
Sema3C	Semaphorin 3C
SEM	Standard error of the mean
SEP	Septum
SNAP25	Synaptosome-associated protein of 25 kDa
SP	Subplate
ST	Striatum
SVZ	Subventricular zone
Venus	Improved version of the YFP
VZ	Ventricular zone
Wnt	Wingless-Int
YFP	Yellow fluorescent protein

Competing interests

The authors declare that they have no competing interests.

Authors' contributions

The author(s) have made the following declarations about their contributions: Conceived and designed the experiments: MN SM CL. Performed the experiments: MN SM DV CD. Analysed the data: MN SM CL. Contributed reagents/materials/analysis tools: FA JPH NR NK TV YY AD. Wrote the paper: SM CL. All authors read and approved the final manuscript.

Funding

Work in the laboratory of C. Lebrand is supported by the Fond National Suisse (FNS 31003A_122550). S. Minocha is supported by a postdoctoral fellowship from the Fondation Pierre Mercier pour la Science. Work in the Kessaris laboratory is supported by a European Research Council (ERC) Starting Grant under the European Community's Seventh Framework Programme (FP7/2007-2013)/ERC Grant agreement no. 207807 and the Wellcome Trust. Work in the lab of Yuchio Yanagawa is supported by the MEXT, Japan and Takeda Science Foundation.

Acknowledgements

We would like to thank F. Thevenaz and Alain Gnecchi for mouse care, plugs and genotyping. We are particularly grateful to Dominique Nicolas for technical assistance. We thank Jean-Yves Chatton from the Cellular Imaging Facility (CIF, University of Lausanne) for imaging assistance. We particularly thank Peter Clarke for the reading and comments on the manuscript.

References:

Anderson, S. A., Eisenstat, D. D., Shi, L. and Rubenstein, J. L. (1997). Interneuron migration from basal forebrain to neocortex: dependence on Dlx genes. *Science* **278**, 474-6.

Anderson, S. A., Kaznowski, C. E., Horn, C., Rubenstein, J. L. and McConnell, S. K. (2002). Distinct origins of neocortical projection neurons and interneurons in vivo. *Cereb Cortex* **12**, 702-9.

Anderson, S. A., Marin, O., Horn, C., Jennings, K. and Rubenstein, J. L. (2001). Distinct cortical migrations from the medial and lateral ganglionic eminences. *Development* **128**, 353-63.

Andrews, W., Liapi, A., Plachez, C., Camurri, L., Zhang, J., Mori, S., Murakami, F., Parnavelas, J. G., Sundaresan, V. and Richards, L. J. (2006). Robo1 regulates the development of major axon tracts and interneuron migration in the forebrain. *Development* **133**, 2243-52.

Andrews, W. D., Barber, M. and Parnavelas, J. G. (2007). Slit-Robo interactions during cortical development. *J Anat* **211**, 188-98.

Bagnard, D., Lohrum, M., Uziel, D., Puschel, A. W. and Bolz, J. (1998). Semaphorins act as attractive and repulsive guidance signals during the development of cortical projections. *Development* **125**, 5043-5053.

Bagri, A., Marin, O., Plump, A. S., Mak, J., Pleasure, S. J., Rubenstein, J. L. and Tessier-Lavigne, M. (2002). Slit proteins prevent midline crossing and determine the dorsoventral position of major axonal pathways in the mammalian forebrain. *Neuron* **33**, 233-248.

Bagri, A. and Tessier-Lavigne, M. (2002). Neuropilins as Semaphorin receptors: in vivo functions in neuronal cell migration and axon guidance. *Adv Exp Med Biol* **515**, 13-31.

Bashaw, G. J. and Klein, R. (2010). Signaling from axon guidance receptors. *Cold Spring Harb Perspect Biol* **2**, a001941.

Batista-Brito, R., Machold, R., Klein, C. and Fishell, G. (2008). Gene expression in cortical interneuron precursors is prescient of their mature function. *Cereb Cortex* **18**, 2306-17.

Benadiba, C., Magnani, D., Niquille, M., Morle, L., Valloton, D., Nawabi, H., Ait-Lounis, A., Otsmane, B., Reith, W., Theil, T. et al. (2012). The ciliogenic transcription factor RFX3 regulates early midline distribution of guidepost neurons required for corpus callosum development. *PLoS Genet* **8**, e1002606.

Borrell, V., Yoshimura, Y. and Callaway, E. M. (2005). Targeted gene delivery to telencephalic inhibitory neurons by directional in utero electroporation. *J Neurosci Methods* **143**, 151-8.

Bush, J. O. and Soriano, P. (2009). Ephrin-B1 regulates axon guidance by reverse signaling through a PDZ-dependent mechanism. *Genes Dev* **23**, 1586-99.

Butt, S. J., Fuccillo, M., Nery, S., Noctor, S., Kriegstein, A., Corbin, J. G. and Fishell, G. (2005). The temporal and spatial origins of cortical interneurons predict their physiological subtype. *Neuron* **48**, 591-604.

Cancedda, L., Fiumelli, H., Chen, K. and Poo, M. M. (2007). Excitatory GABA action is essential for morphological maturation of cortical neurons in vivo. *J Neurosci* **27**, 5224-35.

Castellani, V., De Angelis, E., Kenwrick, S. and Rougon, G. (2002). Cis and trans interactions of L1 with neuropilin-1 control axonal responses to semaphorin 3A. *EMBO J* **21**, 6348-57.
Chedotal, A. (2010). Further tales of the midline. *Curr Opin Neurobiol*.
Chen, G., Sima, J., Jin, M., Wang, K. Y., Xue, X. J., Zheng, W., Ding, Y. Q. and Yuan, X. B. (2008). Semaphorin-3A guides radial migration of cortical neurons during development. *Nat Neurosci* **11**, 36-44.
Choe, Y., Siegenthaler, J. A. and Pleasure, S. J. (2012). A cascade of morphogenic signaling initiated by the meninges controls corpus callosum formation. *Neuron* **73**, 698-712.
Corbin, J. G., Nery, S. and Fishell, G. (2001). Telencephalic cells take a tangent: non-radial migration in the mammalian forebrain. *Nat Neurosci* **4 Suppl**, 1177-82.
Dickson, B. J. (2002). Molecular mechanisms of axon guidance. *Science* **298**, 1959-64.
Dickson, B. J. and Zou, Y. (2010). Navigating intermediate targets: the nervous system midline. *Cold Spring Harb Perspect Biol* **2**, a002055.
Doherty, D., Tu, S., Schilmoeller, K. and Schilmoeller, G. (2006). Health-related issues in individuals with agenesis of the corpus callosum. *Child Care Health Dev* **32**, 333-42.
Egea, J. and Klein, R. (2007). Bidirectional Eph-ephrin signaling during axon guidance. *Trends Cell Biol* **17**, 230-8.
Fazeli, A., Dickinson, S. L., Hermiston, M. L., Tighe, R. V., Steen, R. G., Small, C. G., Stoeckli, E. T., Keino-Masu, K., Masu, M., Rayburn, H. et al. (1997). Phenotype of mice lacking functional Deleted in colorectal cancer (Dcc) gene. *Nature* **386**, 796-804.
Flames, N., Long, J. E., Garratt, A. N., Fischer, T. M., Gassmann, M., Birchmeier, C., Lai, C., Rubenstein, J. L. and Marin, O. (2004). Short- and long-range attraction of cortical GABAergic interneurons by neuregulin-1. *Neuron* **44**, 251-61.
Flames, N., Pla, R., Gelman, D. M., Rubenstein, J. L., Puelles, L. and Marin, O. (2007). Delineation of multiple subpallial progenitor domains by the combinatorial expression of transcriptional codes. *J Neurosci* **27**, 9682-95.
Fogarty, M., Grist, M., Gelman, D., Marin, O., Pachnis, V. and Kessaris, N. (2007). Spatial genetic patterning of the embryonic neuroepithelium generates GABAergic interneuron diversity in the adult cortex. *J Neurosci* **27**, 10935-46.
Garel, S., Marin, F., Mattei, M. G., Vesque, C., Vincent, A. and Charnay, P. (1997). Family of Ebf/Olf-1-related genes potentially involved in neuronal differentiation and regional specification in the central nervous system. *Dev Dyn* **210**, 191-205.
Gelman, D. M., Martini, F. J., Nobrega-Pereira, S., Pierani, A., Kessaris, N. and Marin, O. (2009). The embryonic preoptic area is a novel source of cortical GABAergic interneurons. *J Neurosci* **29**, 9380-9.
Ghanem, N., Yu, M., Long, J., Hatch, G., Rubenstein, J. L. and Ekker, M. (2007). Distinct cis-regulatory elements from the Dlx1/Dlx2 locus mark different progenitor cell populations in the ganglionic eminences and different subtypes of adult cortical interneurons. *J Neurosci* **27**, 5012-22.
Gu, C., Rodriguez, E. R., Reimert, D. V., Shu, T., Fritzsch, B., Richards, L. J., Kolodkin, A. L. and Ginty, D. D. (2003). Neuropilin-1 conveys semaphorin and VEGF signaling during neural and cardiovascular development. *Dev.Cell* **5**, 45-57.
Hallak, J. E., Crippa, J. A., Pinto, J. P., Machado de Sousa, J. P., Trzesniak, C., Dursun, S. M., McGuire, P., Deakin, J. F. and Zuardi, A. W. (2007). Total agenesis of

the corpus callosum in a patient with childhood-onset schizophrenia. *Arq Neuropsiquiatr* **65**, 1216-9.
Halloran, M. C. and Kalil, K. (1994). Dynamic behaviors of growth cones extending in the corpus callosum of living cortical brain slices observed with video microscopy. *J Neurosci* **14**, 2161-77.
Hardan, A. Y., Minshew, N. J. and Keshavan, M. S. (2000). Corpus callosum size in autism. *Neurology* **55**, 1033-6.
Hatanaka, Y., Matsumoto, T., Yanagawa, Y., Fujisawa, H., Murakami, F. and Masu, M. (2009). Distinct roles of neuropilin 1 signaling for radial and tangential extension of callosal axons. *J Comp Neurol* **514**, 215-25.
Heintz, N. (2001). BAC to the future: the use of bac transgenic mice for neuroscience research. *Nat Rev Neurosci* **2**, 861-70.
Hu, Z., Yue, X., Shi, G., Yue, Y., Crockett, D. P., Blair-Flynn, J., Reuhl, K., Tessarollo, L. and Zhou, R. (2003). Corpus callosum deficiency in transgenic mice expressing a truncated ephrin-A receptor. *J Neurosci* **23**, 10963-70.
Hutchins, B. I., Li, L. and Kalil, K. (2010). Wnt/calcium signaling mediates axon growth and guidance in the developing corpus callosum. *Dev Neurobiol*.
Inta, D., Alfonso, J., von Engelhardt, J., Kreuzberg, M. M., Meyer, A. H., van Hooft, J. A. and Monyer, H. (2008). Neurogenesis and widespread forebrain migration of distinct GABAergic neurons from the postnatal subventricular zone. *Proc Natl Acad Sci U S A* **105**, 20994-9.
Islam, S. M., Shinmyo, Y., Okafuji, T., Su, Y., Naser, I. B., Ahmed, G., Zhang, S., Chen, S., Ohta, K., Kiyonari, H. et al. (2009). Draxin, a repulsive guidance protein for spinal cord and forebrain commissures. *Science* **323**, 388-93.
Jones, L., Lopez-Bendito, G., Gruss, P., Stoykova, A. and Molnar, Z. (2002). Pax6 is required for the normal development of the forebrain axonal connections. *Development* **129**, 5041-52.
Jovanov-Milosevic, N., Petanjek, Z., Petrovic, D., Judas, M. and Kostovic, I. (2010). Morphology, molecular phenotypes and distribution of neurons in developing human corpus callosum. *Eur J Neurosci* **32**, 1423-32.
Kalil, K., Li, L. and Hutchins, B. I. (2011). Signaling mechanisms in cortical axon growth, guidance, and branching. *Front Neuroanat* **5**, 62.
Keeble, T. R., Halford, M. M., Seaman, C., Kee, N., Macheda, M., Anderson, R. B., Stacker, S. A. and Cooper, H. M. (2006). The Wnt receptor Ryk is required for Wnt5a-mediated axon guidance on the contralateral side of the corpus callosum. *J Neurosci* **26**, 5840-8.
Kessaris, N., Fogarty, M., Iannarelli, P., Grist, M., Wegner, M. and Richardson, W. D. (2006). Competing waves of oligodendrocytes in the forebrain and postnatal elimination of an embryonic lineage. *Nat Neurosci* **9**, 173-9.
Kimura, S., Hara, Y., Pineau, T., Fernandez-Salguero, P., Fox, C. H., Ward, J. M. and Gonzalez, F. J. (1996). The T/ebp null mouse: thyroid-specific enhancer-binding protein is essential for the organogenesis of the thyroid, lung, ventral forebrain, and pituitary. *Genes Dev* **10**, 60-9.
Kobayakawa, K., Kobayakawa, R., Matsumoto, H., Oka, Y., Imai, T., Ikawa, M., Okabe, M., Ikeda, T., Itohara, S., Kikusui, T. et al. (2007). Innate versus learned odour processing in the mouse olfactory bulb. *Nature* **450**, 503-8.

Lavdas, A. A., Grigoriou, M., Pachnis, V. and Parnavelas, J. G. (1999). The medial ganglionic eminence gives rise to a population of early neurons in the developing cerebral cortex. *J Neurosci* **19**, 7881-8.

Lee, S., Hjerling-Leffler, J., Zagha, E., Fishell, G. and Rudy, B. (2010). The largest group of superficial neocortical GABAergic interneurons expresses ionotropic serotonin receptors. *J Neurosci* **30**, 16796-808.

Lopez-Bendito, G., Cautinat, A., Sanchez, J. A., Bielle, F., Flames, N., Garratt, A. N., Talmage, D. A., Role, L. W., Charnay, P., Marin, O. et al. (2006). Tangential neuronal migration controls axon guidance: a role for neuregulin-1 in thalamocortical axon navigation. *Cell* **125**, 127-42.

Lopez-Bendito, G., Flames, N., Ma, L., Fouquet, C., Di Meglio, T., Chedotal, A., Tessier-Lavigne, M. and Marin, O. (2007). Robo1 and Robo2 cooperate to control the guidance of major axonal tracts in the mammalian forebrain. *J Neurosci* **27**, 3395-407.

Lopez-Bendito, G., Sturgess, K., Erdelyi, F., Szabo, G., Molnar, Z. and Paulsen, O. (2004). Preferential origin and layer destination of GAD65-GFP cortical interneurons. *Cereb Cortex* **14**, 1122-33.

Mann, F., Chauvet, S. and Rougon, G. (2007). Semaphorins in development and adult brain: Implication for neurological diseases. *Prog Neurobiol* **82**, 57-79.

Marin, O. and Rubenstein, J. L. (2001). A long, remarkable journey: tangential migration in the telencephalon. *Nat Rev Neurosci* **2**, 780-90.

Marin, O. and Rubenstein, J. L. (2003). Cell migration in the forebrain. *Annu Rev Neurosci* **26**, 441-83.

Marin, O., Valiente, M., Ge, X. and Tsai, L. H. (2010). Guiding neuronal cell migrations. *Cold Spring Harb Perspect Biol* **2**, a001834.

Mendes, S. W., Henkemeyer, M. and Liebl, D. J. (2006). Multiple Eph receptors and B-class ephrins regulate midline crossing of corpus callosum fibers in the developing mouse forebrain. *J Neurosci* **26**, 882-92.

Metin, C., Baudoin, J. P., Rakic, S. and Parnavelas, J. G. (2006). Cell and molecular mechanisms involved in the migration of cortical interneurons. *Eur J Neurosci* **23**, 894-900.

Miyoshi, G., Hjerling-Leffler, J., Karayannis, T., Sousa, V. H., Butt, S. J., Battiste, J., Johnson, J. E., Machold, R. P. and Fishell, G. (2010). Genetic fate mapping reveals that the caudal ganglionic eminence produces a large and diverse population of superficial cortical interneurons. *J Neurosci* **30**, 1582-94.

Nery, S., Fishell, G. and Corbin, J. G. (2002). The caudal ganglionic eminence is a source of distinct cortical and subcortical cell populations. *Nat Neurosci* **5**, 1279-87.

Nery, S., Wichterle, H. and Fishell, G. (2001). Sonic hedgehog contributes to oligodendrocyte specification in the mammalian forebrain. *Development* **128**, 527-40.

Niquille, M., Garel, S., Mann, F., Hornung, J. P., Otsmane, B., Chevalley, S., Parras, C., Guillemot, F., Gaspar, P., Yanagawa, Y. et al. (2009). Transient neuronal populations are required to guide callosal axons: a role for semaphorin 3C. *PLoS Biol* **7**, e1000230.

Ozaki, H. S. and Wahlsten, D. (1998). Timing and origin of the first cortical axons to project through the corpus callosum and the subsequent emergence of callosal projection cells in mouse. *J Comp Neurol* **400**, 197-206.

Paul, L. K., Brown, W. S., Adolphs, R., Tyszka, J. M., Richards, L. J., Mukherjee, P. and Sherr, E. H. (2007). Agenesis of the corpus callosum: genetic, developmental and functional aspects of connectivity. *Nat Rev Neurosci* **8**, 287-99.

Piper, M., Plachez, C., Zalucki, O., Fothergill, T., Goudreau, G., Erzurumlu, R., Gu, C. and Richards, L. J. (2009). Neuropilin 1-Sema signaling regulates crossing of cingulate pioneering axons during development of the corpus callosum. *Cereb Cortex* **19 Suppl 1**, i11-21.

Plessen, K. J., Gruner, R., Lundervold, A., Hirsch, J. G., Xu, D., Bansal, R., Hammar, A., Lundervold, A. J., Wentzel-Larsen, T., Lie, S. A. et al. (2006). Reduced white matter connectivity in the corpus callosum of children with Tourette syndrome. *J Child Psychol Psychiatry* **47**, 1013-22.

Polleux, F., Morrow, T. and Ghosh, A. (2000). Semaphorin 3A is a chemoattractant for cortical apical dendrites. *Nature* **404**, 567-73.

Rash, B. G. and Richards, L. J. (2001). A role for cingulate pioneering axons in the development of the corpus callosum. *J Comp Neurol* **434**, 147-57.

Ren, T., Anderson, A., Shen, W. B., Huang, H., Plachez, C., Zhang, J., Mori, S., Kinsman, S. L. and Richards, L. J. (2006). Imaging, anatomical, and molecular analysis of callosal formation in the developing human fetal brain. *Anat Rec A Discov Mol Cell Evol Biol* **288**, 191-204.

Ren, T., Zhang, J., Plachez, C., Mori, S. and Richards, L. J. (2007). Diffusion tensor magnetic resonance imaging and tract-tracing analysis of Probst bundle structure in Netrin1- and DCC-deficient mice. *J Neurosci* **27**, 10345-9.

Richards, L. J., Plachez, C. and Ren, T. (2004). Mechanisms regulating the development of the corpus callosum and its agenesis in mouse and human. *Clin Genet* **66**, 276-89.

Riederer, B. M., Berbel, P. and Innocenti, G. M. (2004). Neurons in the corpus callosum of the cat during postnatal development. *Eur J Neurosci* **19**, 2039-46.

Riederer, B. M. and Innocenti, G. M. (1992). MAP2 Isoforms in Developing Cat Cerebral Cortex and Corpus Callosum. *Eur J Neurosci* **4**, 1376-1386.

Rubin, A. N., Alfonsi, F., Humphreys, M. P., Choi, C. K., Rocha, S. F. and Kessaris, N. (2010). The germinal zones of the basal ganglia but not the septum generate GABAergic interneurons for the cortex. *J Neurosci* **30**, 12050-62.

Rudy, B., Fishell, G., Lee, S. and Hjerling-Leffler, J. (2010). Three groups of interneurons account for nearly 100% of neocortical GABAergic neurons. *Dev Neurobiol*.

Rufer, N., Reichenbach, P. and Romero, P. (2005). Methods for the ex vivo characterization of human CD8+ T subsets based on gene expression and replicative history analysis. *Methods Mol Med.* **109**, 265-284.

Sanchez-Camacho, C., Ortega, J. A., Ocana, I., Alcantara, S. and Bovolenta, P. (2011). Appropriate Bmp7 levels are required for the differentiation of midline guidepost cells involved in corpus callosum formation. *Dev Neurobiol* **71**, 337-50.

Seidman, L. J., Valera, E. M. and Makris, N. (2005). Structural brain imaging of attention-deficit/hyperactivity disorder. *Biol Psychiatry* **57**, 1263-72.

Serafini, T., Colamarino, S. A., Leonardo, E. D., Wang, H., Beddington, R., Skarnes, W. C. and Tessier-Lavigne, M. (1996). Netrin-1 is required for commissural axon guidance in the developing vertebrate nervous system. *Cell* **87**, 1001-14.

Shu, T., Li, Y., Keller, A. and Richards, L. J. (2003a). The glial sling is a migratory population of developing neurons. *Development* **130**, 2929-37.

Shu, T., Puche, A. C. and Richards, L. J. (2003b). Development of midline glial populations at the corticoseptal boundary. *J Neurobiol* **57**, 81-94.

Shu, T. and Richards, L. J. (2001). Cortical axon guidance by the glial wedge during the development of the corpus callosum. *J Neurosci* **21**, 2749-58.
Shu, T., Sundaresan, V., McCarthy, M. M. and Richards, L. J. (2003c). Slit2 guides both precrossing and postcrossing callosal axons at the midline in vivo. *J Neurosci* **23**, 8176-84.
Siegenthaler, J. A., Ashique, A. M., Zarbalis, K., Patterson, K. P., Hecht, J. H., Kane, M. A., Folias, A. E., Choe, Y., May, S. R., Kume, T. et al. (2009). Retinoic acid from the meninges regulates cortical neuron generation. *Cell* **139**, 597-609.
Silver, J., Edwards, M. A. and Levitt, P. (1993). Immunocytochemical demonstration of early appearing astroglial structures that form boundaries and pathways along axon tracts in the fetal brain. *J Comp Neurol* **328**, 415-36.
Silver, J. and Ogawa, M. Y. (1983). Postnatally induced formation of the corpus callosum in acallosal mice on glia-coated cellulose bridges. *Science* **220**, 1067-9.
Smith, K. M., Ohkubo, Y., Maragnoli, M. E., Rasin, M. R., Schwartz, M. L., Sestan, N. and Vaccarino, F. M. (2006). Midline radial glia translocation and corpus callosum formation require FGF signaling. *Nature Neuroscience* **9**, 787-797.
Speiser, D. E., Baumgaertner, P., Barbey, C., Rubio-Godoy, V., Moulin, A., Corthesy, P., Devevre, E., Dietrich, P. Y., Rimoldi, D., Lienard, D. et al. (2006). A novel approach to characterize clonality and differentiation of human melanoma-specific T cell responses: spontaneous priming and efficient boosting by vaccination. *J Immunol.* **177**, 1338-1348.
Srinivas, S., Watanabe, T., Lin, C. S., William, C. M., Tanabe, Y., Jessell, T. M. and Costantini, F. (2001). Cre reporter strains produced by targeted insertion of EYFP and ECFP into the ROSA26 locus. *BMC Dev Biol* **1**, 4.
Stoeckli, E. T. and Landmesser, L. T. (1998). Axon guidance at choice points. *Curr Opin Neurobiol* **8**, 73-9.
Stuhmer, T., Anderson, S. A., Ekker, M. and Rubenstein, J. L. (2002). Ectopic expression of the Dlx genes induces glutamic acid decarboxylase and Dlx expression. *Development* **129**, 245-52.
Sussel, L., Marin, O., Kimura, S. and Rubenstein, J. L. (1999). Loss of Nkx2.1 homeobox gene function results in a ventral to dorsal molecular respecification within the basal telencephalon: evidence for a transformation of the pallidum into the striatum. *Development* **126**, 3359-70.
Suter, D. M. and Forscher, P. (2000). Substrate-cytoskeletal coupling as a mechanism for the regulation of growth cone motility and guidance. *J Neurobiol* **44**, 97-113.
Tamamaki, N., Yanagawa, Y., Tomioka, R., Miyazaki, J., Obata, K. and Kaneko, T. (2003). Green fluorescent protein expression and colocalization with calretinin, parvalbumin, and somatostatin in the GAD67-GFP knock-in mouse. *J Comp Neurol* **467**, 60-79.
Vitalis, T. and Rossier, J. (2010). New insights into cortical interneurons development and classification: Contribution of developmental studies. *Dev Neurobiol*.
Vucurovic, K., Gallopin, T., Ferezou, I., Rancillac, A., Chameau, P., van Hooft, J. A., Geoffroy, H., Monyer, H., Rossier, J. and Vitalis, T. (2010). Serotonin 3A receptor subtype as an early and protracted marker of cortical interneuron subpopulations. *Cereb Cortex* **20**, 2333-47.
Wichterle, H., Turnbull, D. H., Nery, S., Fishell, G. and Alvarez-Buylla, A. (2001). In utero fate mapping reveals distinct migratory pathways and fates of neurons born in the mammalian basal forebrain. *Development* **128**, 3759-71.

Wilkinson, D. G. (2001). Multiple roles of EPH receptors and ephrins in neural development. *Nat Rev Neurosci* **2**, 155-64.
Xu, Q., Cobos, I., De La Cruz, E., Rubenstein, J. L. and Anderson, S. A. (2004). Origins of cortical interneuron subtypes. *J Neurosci* **24**, 2612-22.
Yazdani, U. and Terman, J. R. (2006). The semaphorins. *Genome Biol* **7**, 211.
Yu, T. W. and Bargmann, C. I. (2001). Dynamic regulation of axon guidance. *Nat Neurosci* **4 Suppl**, 1169-76.
Zhao, H., Maruyama, T., Hattori, Y., Sugo, N., Takamatsu, H., Kumanogoh, A., Shirasaki, R. and Yamamoto, N. (2011). A molecular mechanism that regulates medially oriented axonal growth of upper layer neurons in the developing neocortex. *J Comp Neurol* **519**, 834-48.

Figure legends:

Figure 1. ***Organization and birthdating of CC guidepost GABAergic neurons during embryonic development***

(A-E) Single immunohistochemistry for GFP **(A1-E1)** and double immunohistochemistry for GFP and L1 **(A2-E2)** in coronal sections from *GAD67-GFP* mice at E14.5 **(A1-A2)**, E16.5 **(B1-B2),** E18.5 **(C1-C2)**, P7 **(D1-D2)** and P14 **(E1-E2)**. **A2** to **E2** are higher power views of the CC seen in **A1** to **E1 (**open arrows**)**, respectively. **(A1-E1** and **A2-E2)** Cell nuclei were counterstained in blue with Hoechst. At E14.5, GAD67-GFP$^+$ neurons are migrating in the white matter below the frontal cortex **(CFr) (A1)** while callosal axons approach the midline at the corticoseptal boundary **(CSB) (A2**, arrowheads**)**. At E16.5, pioneering axons grow through GAD67-GFP$^+$ neurons that invade the lateral **(B1)** and medial **(B2)** part of the CC. At E18.5, commissural axons are delimited by GAD67-GFP$^+$ neurons that are dispersed in the entire CC white matter **(C1** and **C2)** and form a cluster of cells in the wings of the CC **(C1, *)**. At P7, GAD67-GFP$^+$ neurons have progressively disappeared from the CC and its wings **(*) (D1-D2)**. At P14, only few GAD67-GFP$^+$ neurons remain in the callosal track **(E1-E2)**.

(F-J) Double immunohistochemistry for GFP and 5-bromo2'-deoxy-uridine (BrdU) in coronal sections from *GAD67-GFP* mice at E16.5 injected at E12.5 **(F1-F2)** or E14.5 **(G1-G2)** and from *GAD67-GFP* mice at E18.5 injected at E12.5 **(H1-H2)**, E14.5 **(I1-I2)**, or E16.5 **(J1-J2)**. **F2** to **J2**: higher power views of the CC seen in **F1** to **J1 (**open arrows**)**, respectively. Insets in **F2** to **J2** are high magnified zones of CC regions indicated by white arrowheads. **(F1-G1)** At E16.5, most GABAergic guidepost neurons of the CC are born at E12.5 since colocalization between GFP and BrdU is visible primarily when injections are done at E12.5 **(F2**, open arrowheads and inset**)**. **(H1-J1)** Later at E18.5, the bulk of CC GABAergic guidepost neurons are generated from E12.5 to E14.5 since numerous GAD67-GFP$^+$/BrdU$^+$ cells are visualized after E12.5 and E14.5 injections **(H2** and **I2**, open arrowheads and insets**)** but nearly none after E16.5 injections **(J2**, inset**)**.

(K) Graphical representation displaying the percentage of neurons positive for both BrdU and GAD67-GFP compared to the total number of GAD67-GFP+ neurons in the medial zone (grey bars) and lateral zone (black bars) of the CC in E16.5 brains injected at E12.5 or E14.5 and in E18.5 brains injected at E12.5, E14.5, or E16.5.

(CCi) cingulate cortex; **(CPa)** parietal cortex; **(IG)** induseum griseum; **(LGE)** lateral ganglionic eminence; **(LV)** lateral ventricle; **(SEP)** septum; **(ST)** striatum.

Bar = 485 µm in F1, G1; 435 µm in A1, B1, C1, D1, E1; 220 µm in H1, I1, J1; 110 µm in A2, B2, C2, D2, E2, H2, I2, J2; 75 µm in F2 and 50 µm in G2.

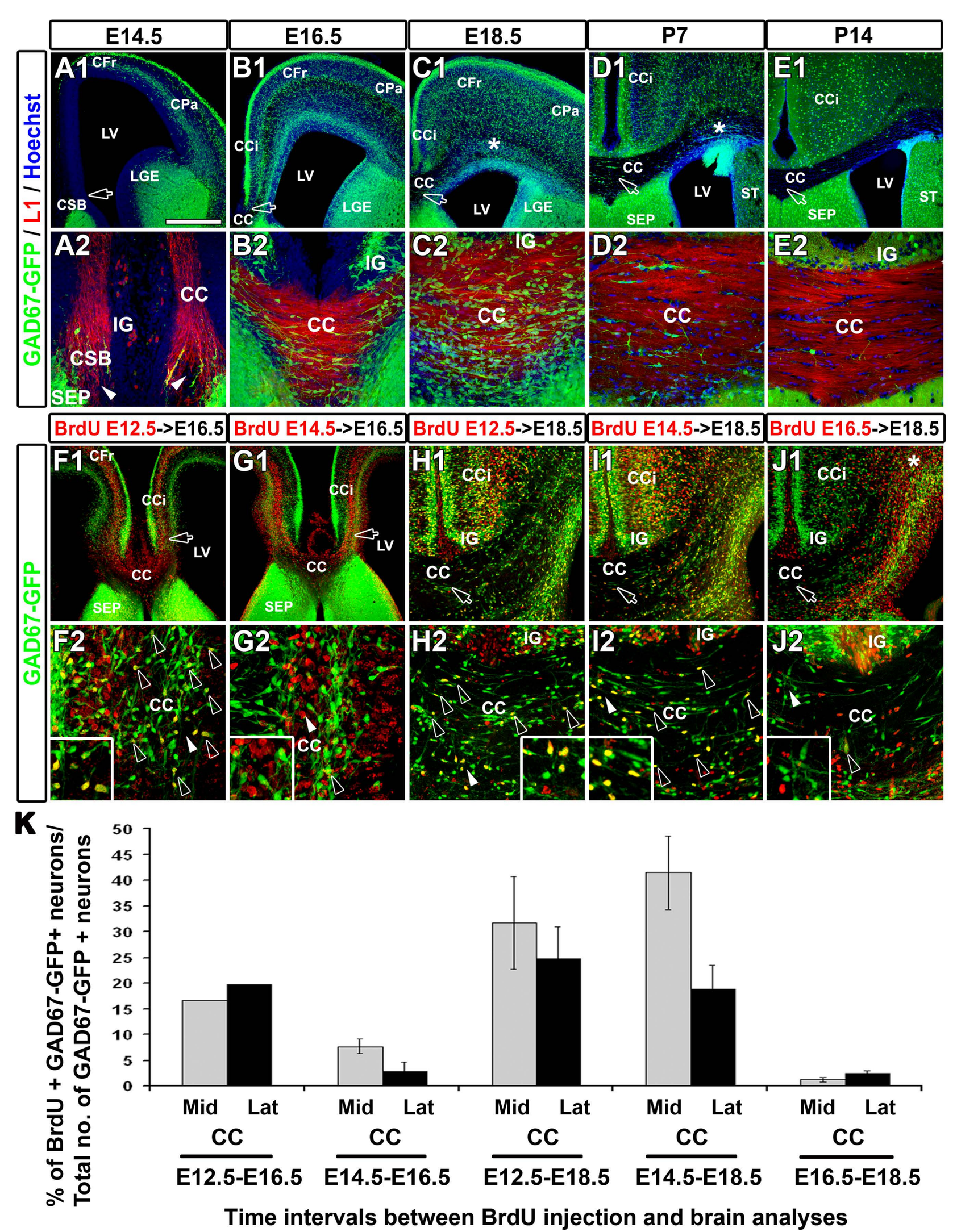
E14.5
E16.5
E18.5
P7
P14
GAD67-GFP / L1 / Hoechst
A1
CFr
CPa
LV
LGE
CSB
B1
CCi
CC
C1
D1
E1
A2
IG
SEP
B2
C2
D2
E2
BrdU E12.5->E16.5
BrdU E14.5->E16.5
BrdU E12.5->E18.5
BrdU E14.5->E18.5
BrdU E16.5->E18.5
GAD67-GFP
F1
G1
H1
I1
J1
F2
G2
H2
I2
J2
K
% of BrdU + GAD67-GFP+ neurons/
Total no. of GAD67-GFP + neurons
50
45
40
35
30
25
20
15
10
5
0
Mid
Lat
CC
E12.5-E16.5
E14.5-E16.5
E12.5-E18.5
E14.5-E18.5
E16.5-E18.5
Time intervals between BrdU injection and brain analyses

Figure 2. ***The MGE but not the LGE is a source of CC GABAergic guidepost neurons***
(A1) Experimental paradigms used to determine whether CC GABAergic neurons originate from the LGE or the MGE. To test this hypothesis, small explants of E14.5 GAD67-GFP$^+$ LGE and MGE containing GABAergic neuron precursors are transplanted in the corresponding zones of unlabelled host slices selected at the level where the CC main body forms. **(A2)** GFP signal showing that LGE-derived GAD67-GFP$^+$ neurons mainly migrate in the striatal mantle, while MGE-derived GAD67-GFP$^+$ neurons massively migrate to the cortex and the CC white matter.
(B) Use of *in vitro* electroporation to determine whether CC GABAergic neurons originate from the LGE or the MGE. LGE **(C)** as well as MGE **(D1)** of E14.5 coronal telencephalic GAD67-GFP$^+$ slices were focally electroporated with a plasmid (*pCAG-IRES-Tomato)* expressing the red fluorescent protein Tomato. **(C)** After focal LGE electroporation, LGE progenitors gave rise to GAD67-GFP$^+$ neurons labeled in red for the tomato that have migrated in the striatal mantle. **(D1)** After focal MGE electroporation, MGE precursors generated GAD67-GFP$^+$/Tomato$^+$ neurons that have migrated within the CC **(D2,** arrowheads**)**.
(E1) Experimental paradigms used to ascertain the MGE origin of CC GABAergic neurons. To this end, Nkx2.1 staining specific for the MGE region was performed after electroporating a GFP expressing plasmid (*pCAG-GFP*) into the presumptive MGE **(*)** of E14.5 coronal telencephalic slices. **(E2** and **E3)** Several migrating GFP+ neurons labelled for Nkx2.1 are visualized into the striatum anlage confirming the MGE nature of the electroporated site. **(E4)** Numerous GFP$^+$ GABAergic interneurons originating from the MGE are present through the CC white matter. In accordance with the literature these neurons have stopped to express the Nkx2.1 transcription factor while migrating to the dorsal telencephalon. **A2**, **C**, **D1**, **D2**, **E2** and **E4** Cell nuclei were counterstained in blue with Hoechst. **(CFr)** frontal cortex; **(CPa)** parietal cortex; **(LV)** lateral ventricle.
Bar = 1450 µm in A2; 485 µm in C, D1, E2; 60 µm in E3; 40 µm in E4 and 25 µm in D2.

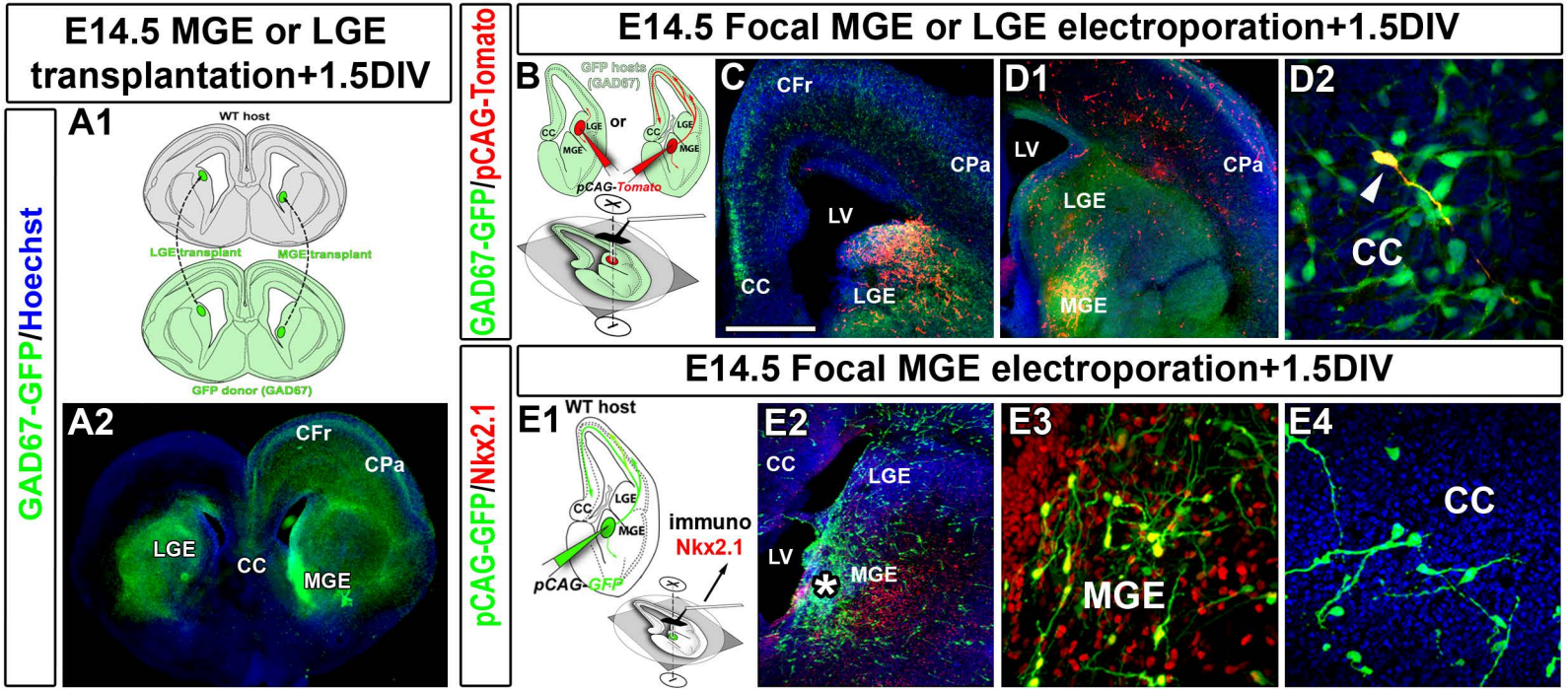
E14.5 MGE or LGE transplantation+1.5DIV
GAD67-GFP/Hoechst
A1
WT host
LGE transplant
MGE transplant
GFP donor (GAD67)
A2
CFr
CPa
LGE
CC
MGE
GAD67-GFP/pCAG-Tomato
E14.5 Focal MGE or LGE electroporation+1.5DIV
B
GFP hosts (GAD67)
or
CC
LGE
MGE
pCAG-Tomato
C
CFr
CPa
LV
CC
LGE
D1
LV
CPa
LGE
MGE
D2
CC
pCAG-GFP/Nkx2.1
E14.5 Focal MGE electroporation+1.5DIV
E1
WT host
CC
LGE
MGE
pCAG-GFP
immuno
Nkx2.1
E2
CC
LGE
LV
MGE
E3
MGE
E4
CC

Figure 3. ***The MGE and the CGE generate CC GABAergic neurons***

Immunohistochemistry for GFP on E16.5 **(A1-A2**, **E1-E2**, **I1-I2** and **M1-M2)** and on E18.5 **(D1-D2**, **H1-H2**, **L1-L2** and **P1-P2)** coronal sections from *GAD67-GFP* **(A1-A2** and **D1-D2)**, *Lhx6-Cre/Rosa26R-YFP* **(E1-E2** and **H1-H2)**, *Nkx2.1-Cre/Dlx1-lox-Venus-lox* **(I1-I2** and **L1-L2)** and *5-HTR3a-GFP* **(M1-M2** and **P1-P2)** mice. **A2**, **D2**, **E2**, **H2**, **I2**, **L2, M2** and **P2** are magnified views of the lateral CC regions visualized in **A1**, **D1**, **E1**, **H1**, **I1**, **L1**, **M1** and **P1**, respectively. All sections were counterstained with Hoechst that labels cell nuclei in blue. Genetic fate mapping analyses indicate that, at E16.5 and E18.5, the CC comprises numerous GAD67-GFP$^+$ neurons, MGE-derived YFP$^+$ GABAergic neurons visualized in *Lhx6-Cre/Rosa26R-YFP* sections, as well as, LGE/CGE-derived Venus$^+$ GABAergic neurons visualized in *Nkx2.1-Cre/Dlx1- Venus^{fl}* sections. In addition, the use of *5-HTR3a-GFP* mice that selectively labels CGE-derived GABAergic neurons confirms the presence of multiple CC GABAergic neurons originating from the CGE and strongly suggests that the LGE/CGE Venus$^+$ neuronal population principally originates from the CGE. **(CCi)** cingulate cortex; **(CFr)** frontal cortex; **(HIC)** hippocampal commissure; **(IG)** induseum griseum; **(IZ)** intermediate zone; **(LV)** lateral ventricle; **(SEP)** septum; **(SP)** subplate; **(SVZ)** subventricular zone; **(VZ)** ventricular zone.

(B and **C)** Bars (means ± SEM) represent the density of all CC GABAergic neurons labelled with the GAD67-GFP and present within the medial **(**mid**)**, lateral **(**lat**)** and entire **(**tot**)** CC of E16.5 **(B)** and of E18.5 **(C)** *GAD67-GFP* mice. **(F** and **G)** Bars (means ± SEM) represent the density of MGE-derived YFP$^+$ neurons present within the medial, lateral and entire CC of E16.5 **(F)** and of E18.5 **(G)** *Lhx6-Cre/Rosa26R-YFP* mice. **(J** and **K)** Bars (means ± SEM) represent the density of LGE/CGE-derived Venus$^+$ neurons that populate the medial, lateral and entire CC of E16.5 **(J)** and of E18.5 **(K)** *Nkx2.1-Cre/Dlx1- Venus^{fl}* embryos. **(N** and **O)** Bars represent the density of CGE-derived 5-HTR3a-GFP$^+$ neurons that occupy the medial, lateral and entire CC of E16.5 **(N)** and of E18.5 **(O)** *5-HTR3a-GFP* embryos. **(B-C, F-G, J-K** and **N-O)** After quantification, the density of all neuronal populations is significantly higher in the lateral CC compare to the medial CC at E16.5 **(*****green lines**)**.** At E18.5, both part of the CC contain the same density of neurons for each population. At E18.5 compare to E16.5, there is a significant increase of overall neuronal population density in the medial CC **(******* red lines**)**.** This occurs at the expense of the lateral CC where the neuronal density for all populations is decreased after the neurons migrate to the medial CC. **(J-K** and **N-O)** In addition the density of the total LGE/CGE and CGE neurons is significantly increased at E18.5 in the entire CC **(**red lines**)**.

Bar = 485 µm in E1, H1, I1, L1, M1, P1; 435 µm in A1, D1; 110 µm in A2, D2 and 60 µm in E2, H2, I2, L2, M2, P2.

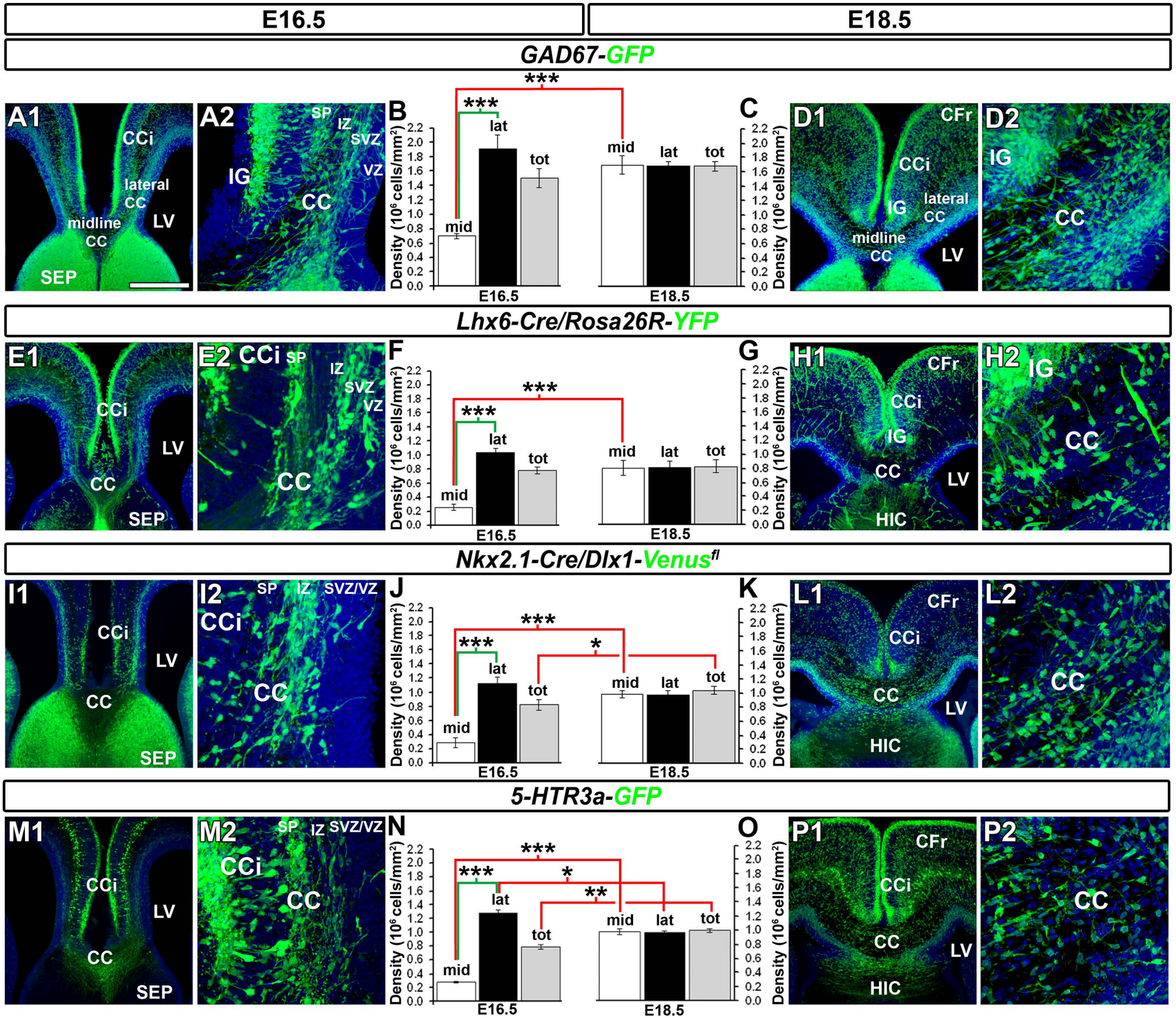
E16.5
E18.5
GAD67-GFP
A1
CCi
lateral CC
midline CC
LV
SEP
A2
SP
IZ
SVZ
VZ
IG
CC
B
C
***
lat
tot
mid
Density (10⁶ cells/mm²)
E16.5
E18.5
D1
CFr
CCi
IG
lateral CC
midline CC
LV
D2
IG
CC
Lhx6-Cre/Rosa26R-YFP
E1
CCi
LV
CC
SEP
E2
CCi
SP
IZ
SVZ
VZ
CC
F
G
*
H1
CFr
CCi
IG
CC
LV
HIC
H2
IG
CC
Nkx2.1-Cre/Dlx1-Venusfl
I1
CCi
LV
CC
SEP
I2
SP
IZ
SVZ/VZ
CCi
CC
J
K
L1
CFr
CCi
CC
LV
HIC
L2
CC
5-HTR3a-GFP
M1
CCi
LV
CC
SEP
M2
SP
IZ
SVZ/VZ
CCi
CC
N
O
**
P1
CFr
CCi
CC
LV
HIC
P2
CC

Figure 4. ***Reduced motility of CC GABAergic guidepost neurons after E16.5***
In vitro time-lapse sequences over a period of around three hours (sequential pictures taken at regular intervals) of GAD67-GFP$^+$ neuron dynamics in coronal CC slices of E14.5 **(A1-A6)** and E16.5 **(B1-B6)** GAD67-GFP$^+$ transgenic mice. Open arrowheads indicate the progression of neurons between sequential pictures while arrowheads highlight immobilized neurons. **(A1-A6)** At E14.5, the majority of the GAD67-GFP$^+$ neurons exhibit rapid movements within the white matter of the CC (open arrowheads). **(B1-B6)** By contrast, at E16.5, nearly all the GAD67-GFP$^+$ neurons exhibit a reduced motility within the white matter of the CC **(**arrowheads**)**. **(C** and **D)** Traces followed by GAD67-GFP$^+$ CC neurons after 5 hrs of time lapse recording are represented in yellow at E14.5 **(C)** and E16.5 **(D)**. **(E)** The basal rate of migration and frequency of neuron pauses per hour in the CC are shown at E14.5, E16.5 and E17.5 (mean ± S.E.M from samples of 70 neurons at E14.5, of 70 neurons at E16.5 and of 35 neurons at E17.5). ***$P < 0.001$; **Ξ** > 0.05; comparison between values obtained at different embryonic ages and done in similar portions of the CC. **(CCi)** cingulate cortex; **(IG)** induseum griseum; **(LGE)** lateral ganglionic eminence; **(LV)** lateral ventricle.
Bar = 485 µm in B1; 240 µm in A1, C, D and 55 µm in A2, A3, A4, A5, A6, B2, B3, B4, B5, B6.

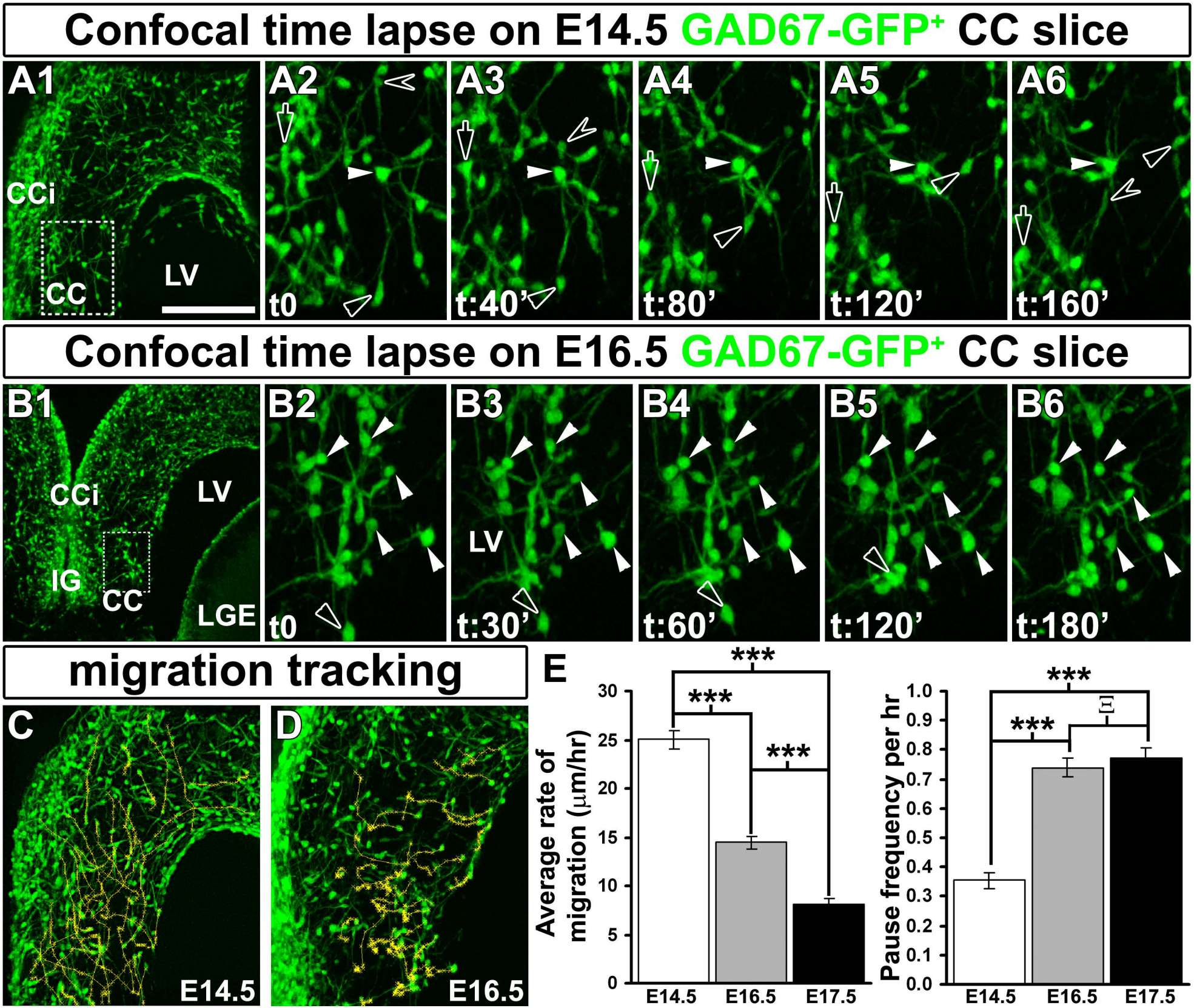
Confocal time lapse on E14.5 GAD67-GFP+ CC slice
A1
CCi
CC
LV
A2
t0
A3
t:40'
A4
t:80'
A5
t:120'
A6
t:160'
Confocal time lapse on E16.5 GAD67-GFP+ CC slice
B1
CCi
LV
IG
CC
LGE
B2
t0
B3
LV
t:30'
B4
t:60'
B5
t:120'
B6
t:180'
migration tracking
C
E14.5
D
E16.5
E
Average rate of migration (μm/hr)
30
25
20
15
10
5
0
***
***
***
E14.5
E16.5
E17.5
Pause frequency per hr
1.0
0.9
0.8
0.7
0.6
0.5
0.4
0.3
0.2
0.1
0.0
***
***
¤
E14.5
E16.5
E17.5

Figure 5. ***Dynamic interactions between CC GABAergic neurons and callosal axons between E16.5 to E18.5.***

(A) Experimental paradigm used to study cell interactions between callosal pioneering axons labelled with the red fluorescent protein Tomato and GAD67-GFP$^+$ CC neurons. For this purpose, a plasmid encoding the Tomato (*pCAG-Ires-Tomato*) was electroporated into the dorsal pallium of E14.5 GAD67-GFP$^+$ living embryos to label neuronal precursors of pyramidal neurons that migrate to the cortex and differentiate for a part into callosal projecting neurons. DNA solution containing the *pCAG-Ires-Tomato* plasmid was pressure-injected focally into the lateral ventricle of E14.5 embryos. Each embryo, while still within the uterine horn, was placed between tweezers-type electrodes. After *in utero* electroporation, the embryos were quickly placed back into the abdominal cavity and allowed to develop until E16.5.

(B1 and **B2)** *In vitro* time-lapse sequences over a period of 100 minutes (at 20 minute intervals) of Tomato-labelled callosal axons and GAD67-GFP$^+$ neurons on coronal CC slices of E16.5 GAD67-GFP$^+$ embryos. **(B1)** Low power view of the CC showing the region of interest where the video imaging was done. **(B2)** High power views of Tomato$^+$ callosal axon growing through the CC and making branch extensions and retractions at different time points **(**t:0 min-t:100 min**)**. Callosal axon branches are seen to make multiple contacts with CC GAD67-GFP+ guidepost neurons **(**t:20 min, t:60 min and t:100 min, arrowheads**)**. Contacts either promote axonal growth **(**t:20 min -t:60 min**)** or lead to growth cone retraction **(**t.80 min -t:100 min**)** and formation of a new branch **(**t:80 min - t:100 min, open arrowhead**)**. **(B3)** Illustration of the iso-surfaces obtained from the GAD67-GFP and live Tomato staining in **B2 (**t:20 min**)**, respectively.

(C) Graphical representation displaying the frequency of axonal extension, branching, retraction and pauses per hour for the Tomato-labelled callosal axons that contact CC GAD67-GFP+ neurons (contact) and for those that do not contact CC GAD67-GFP+ neurons (non-contact) for time-lapse sequence over a period of 180 minutes made at 20 minute intervals $*P < 0.05$; comparison between values obtained for axons making contact or not and done in similar portions of E16.5 CC (samples of 10 axons for each case). Axons making contacts make relatively more branching and pauses than axons that do not contact neurons. Interestingly, callosal axons that contact CC GABAergic neurons extend significantly more than those that do make contact.

(D1 and **D2)** Confocal time-lapse imaging of DiI-labelled callosal axons and GAD67-GFP$^+$ neurons on coronal CC slices of E16.5 *GAD67-GFP* mice. **(D1)** Low power view of the CC showing the region of interest where the video recording was done. **(D2)** High power views of DiI-labelled callosal axons growing along CC GAD67-GFP$^+$ neurons taken at various time points **(**t:0 min, t:30 min, t:60 min**)**. **(E1** and **E2)** Illustration of the iso-surfaces obtained from the GAD67-GFP and live DiI staining in **D1** and **D2**, respectively. White color highlights contact between axons and neurons, and stars indicate neurons that remain immobile. **(IG)** induseum griseum.

Bar = 240 µm in B1, 110 µm in D1, E1, 15 µm in B2 and 30µm in B3, D2, E2.

In utero electroporation of callosal projecting neurons

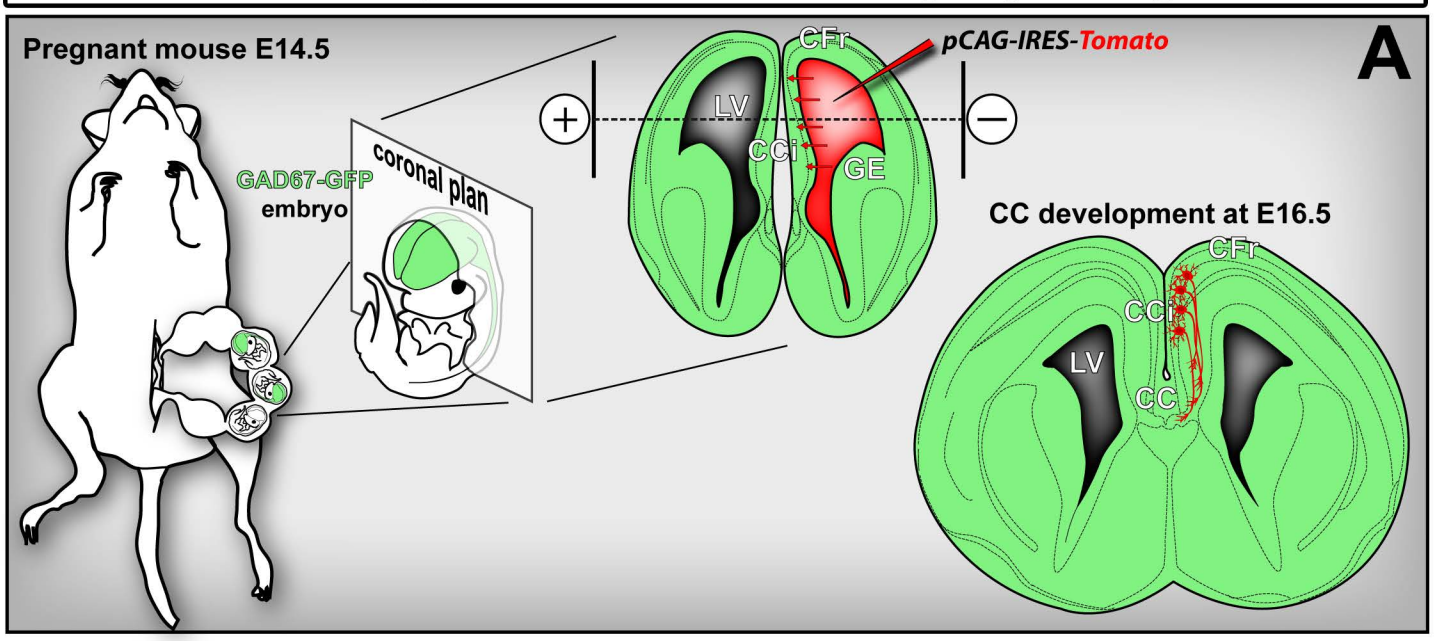

E16.5+1DIV/GAD67-GFP/Tomato+ callosal axons

Region of interest

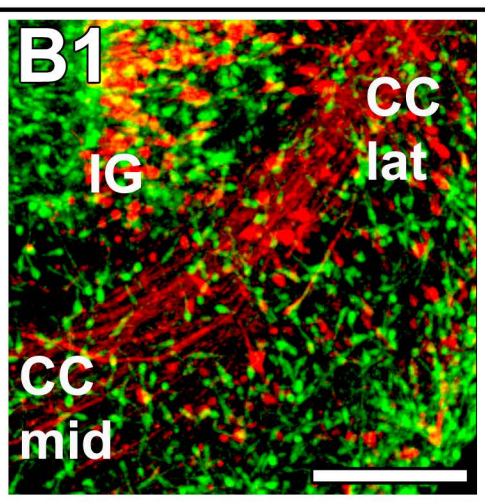

iso-surfaces

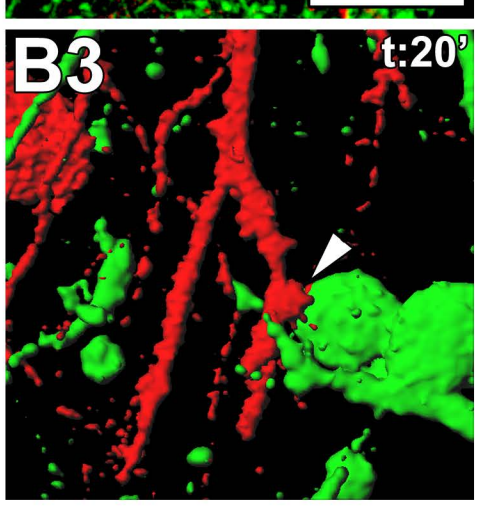

Time-lapse sequence

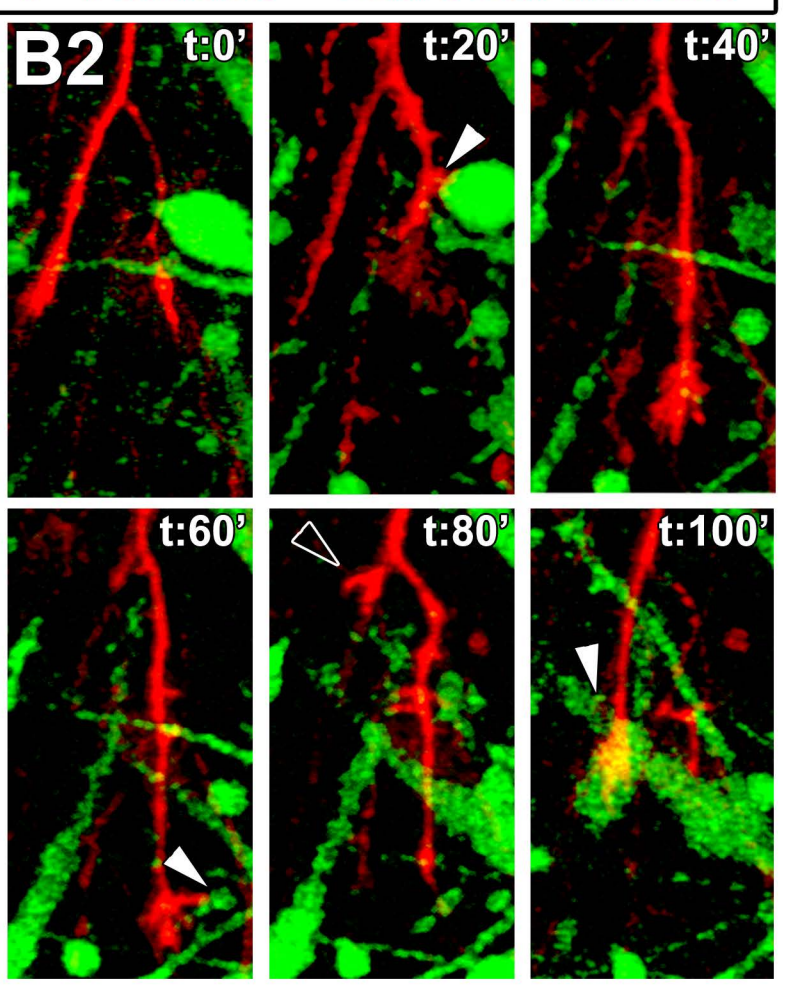

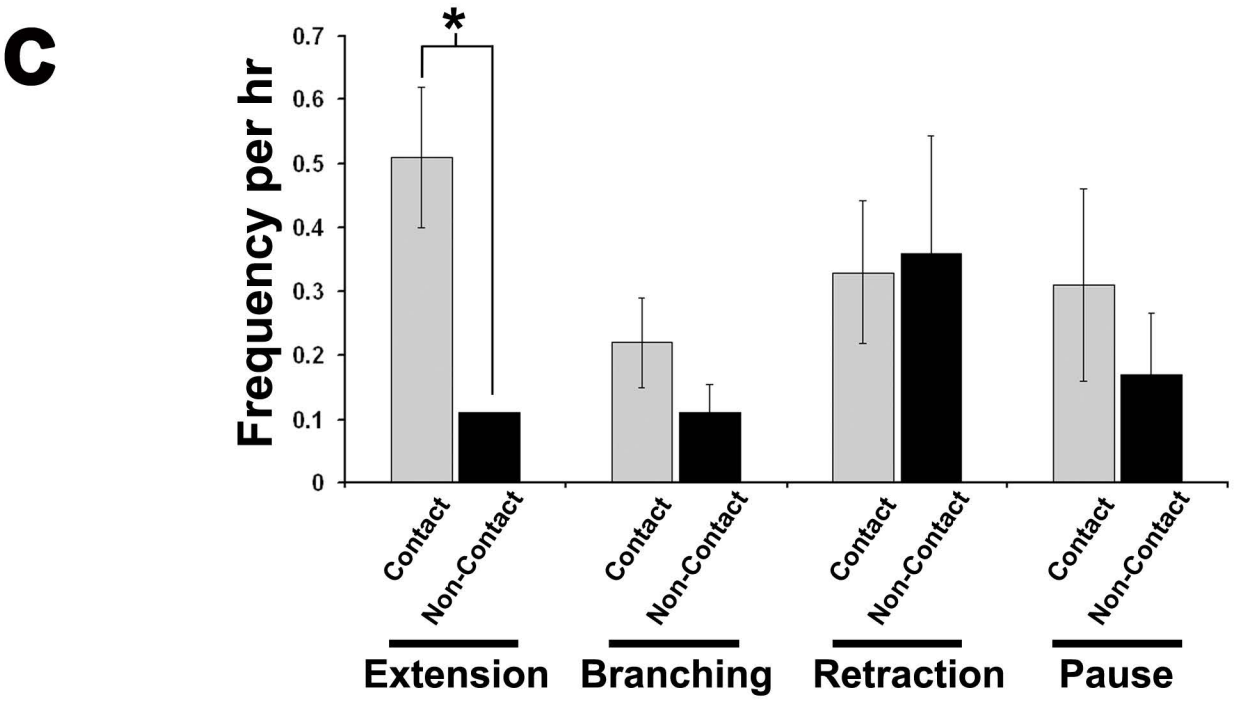

E18.5+1DIV/GAD67-GFP/DiI+ callosal axons

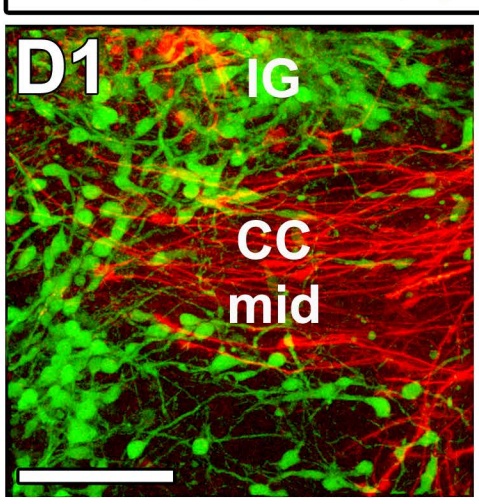

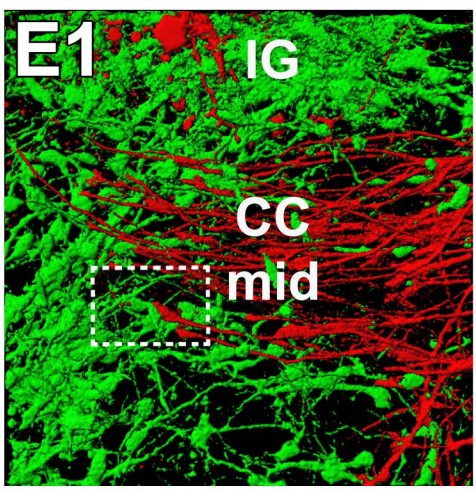

Fluorescence

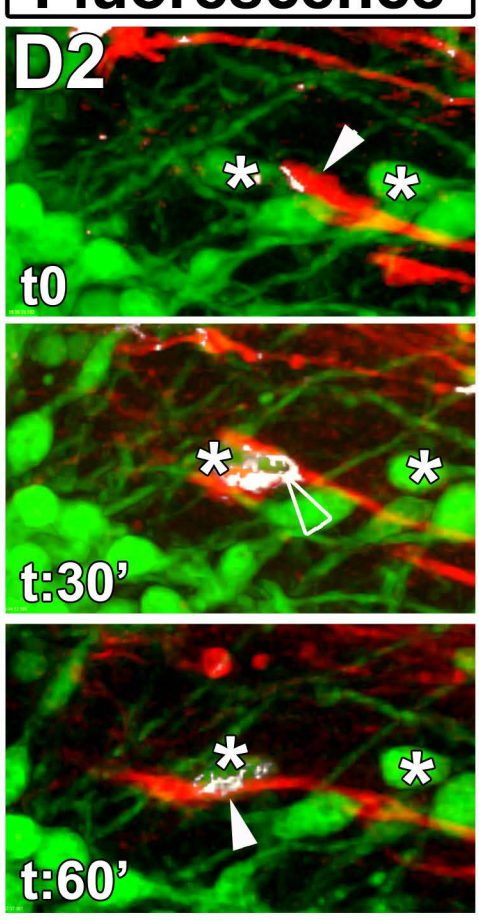

Iso-surfaces

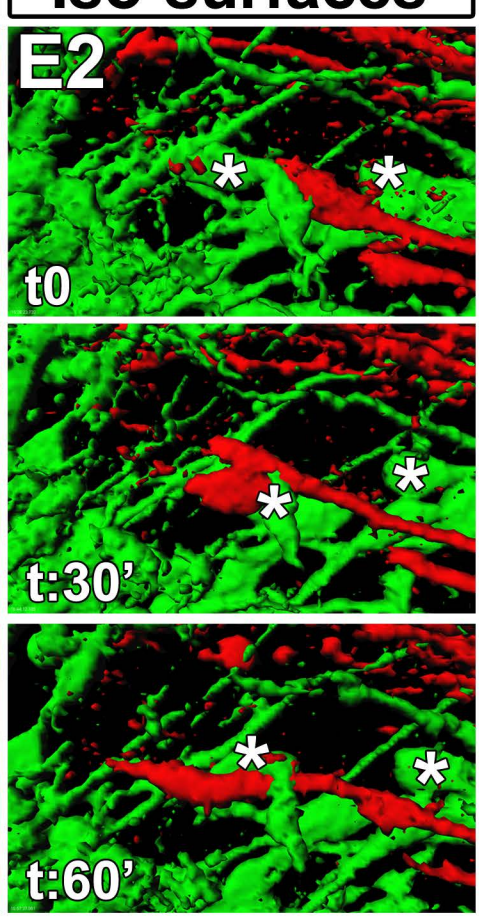

Figure 6. Branching and outgrowth defects in the callosal axons of *Nkx2.1$^{-/-}$:GAD67-GFP* mice brains.

(**A** and **B**) A *pCAG-Ires-Tomato* plasmid was injected into the lateral ventricle and electroporated into the dorsal pallium, to label the callosal projecting neurons, of E14.5 *GAD67-GFP*$^{+}$ living embryos that were allowed to develop until E18.5. Double immunohistochemistry for the GFP and the tomato on CC coronal sections from *Nkx2.1$^{+/+}$:GAD67-GFP*$^{+}$ **(A)** and *Nkx2.1$^{-/-}$:GAD67-GFP*$^{+}$ **(B)** mice brains at E18.5. Cell nuclei were counterstained in blue with Hoechst. The general callosal axon navigation seems to be preserved in the mutants compared to WT brains (compare **B** with **A**). Postcross **(A2, B2)** and midline panels **(A3, B3)** are showing higher magnifications of the callosal axons (in red) and the *GAD67-GFP*$^{+}$ interneurons (in green). In the *Nkx2.1$^{-/-}$:GAD67-GFP*$^{+}$ CC, there was a loss of *GAD67-GFP*$^{+}$ neurons and the axons were not properly fasciculated and made aberrant branches that extended in wrong directions (open arrowheads). (**C**-**D**) High power views of *in vitro* time-lapse sequences over a period of 120 minutes (at 20 minute intervals) of Tomato-labelled callosal axons and GAD67-GFP^{+} neurons on coronal CC slices of E16.5 *Nkx2.1$^{+/+}$:GAD67-GFP*$^{+}$ **(C)** and *Nkx2.1$^{-/-}$:GAD67-GFP*$^{+}$ **(D)** embryos. In the *Nkx2.1$^{-/-}$* brains, though the callosal axons progressed along normal path, they displayed disoriented branch extensions. The diferent trajectories of WT and *Nkx2.1$^{-/-}$* axons within the CC is illustrated by cell tracking paths (E and F, highlighted in white) and 3 sequential pictures (C and D). (G and H) Graphical representation displaying the axonal outgrowth and the distance from the origin per hour for the WT and *Nkx2.1$^{-/-}$* Tomato-labelled callosal axons for time-lapse sequence over a period of 5 hours made at 20 minute intervals ***$P < 0.001$; comparison between values obtained for WT and *Nkx2.1$^{-/-}$* axons (samples of 7 axons for each case). Quantification reveals that while axons in WT and *Nkx2.1$^{-/-}$* axons grow at the same speed, *Nkx2.1$^{-/-}$* axons slowly move away from the origin due to many back and forward movements. **(CC)** corpus callosum; **(CCi)** cingulate cortex; (CFr) frontal cortex; **(IG)** indusium griseum; **(LV)** lateral ventricle; **(SEP)** septum.

Bar = 500 µm in **A** and **B**; 40 µm in postcross (A2, B2) and midline panels (A3, B3); 25 µm in **C** and **D**.

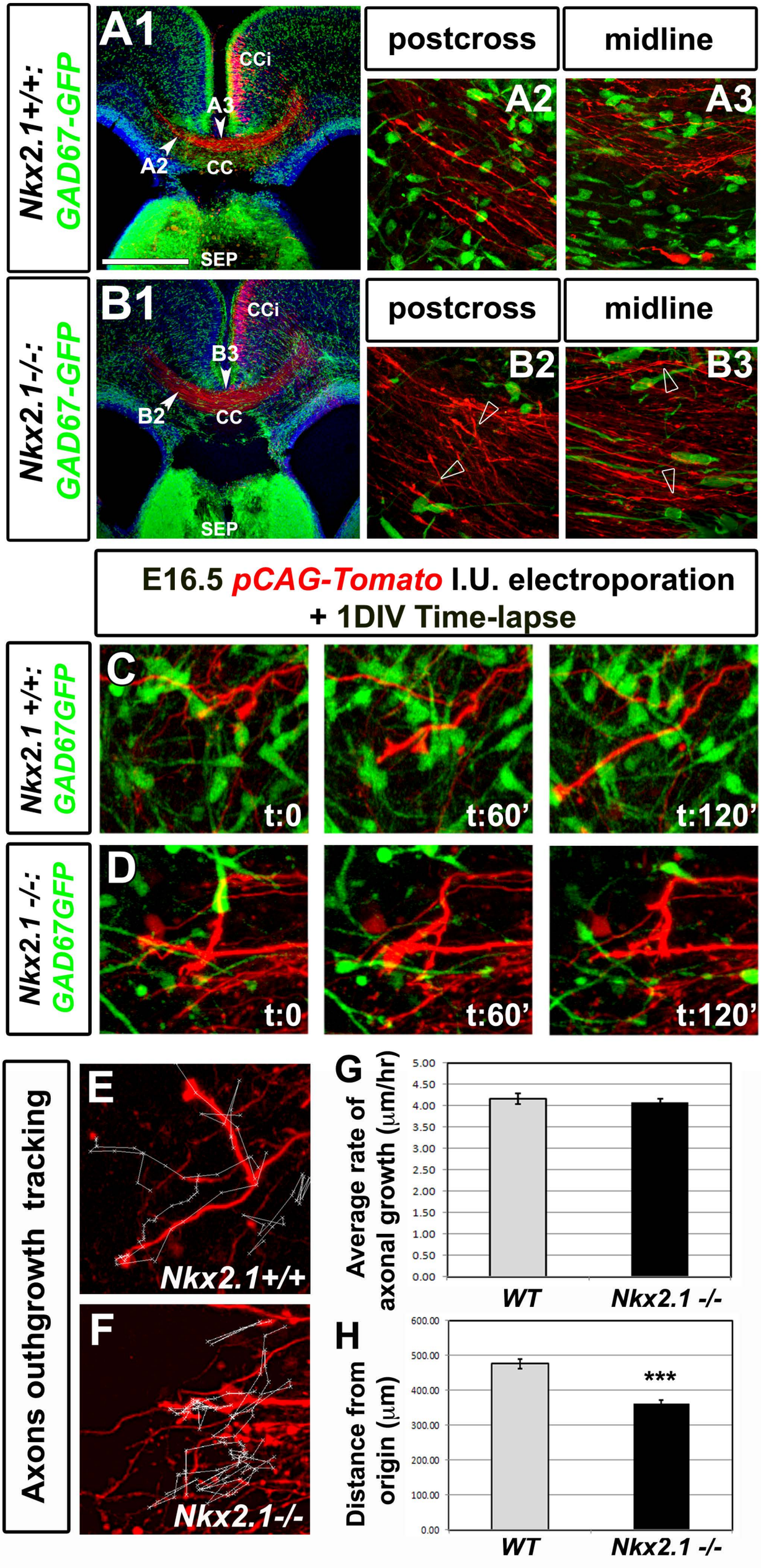
Nkx2.1+/+: GAD67-GFP
A1
CCi
A3
A2
CC
SEP
postcross
midline
A2
A3
Nkx2.1-/-: GAD67-GFP
B1
CCi
B3
B2
CC
SEP
postcross
midline
B2
B3
E16.5 pCAG-Tomato I.U. electroporation
+ 1DIV Time-lapse
Nkx2.1 +/+: GAD67GFP
C
t:0
t:60'
t:120'
Nkx2.1 -/-: GAD67GFP
D
t:0
t:60'
t:120'
Axons outhgrowth tracking
E
Nkx2.1+/+
F
Nkx2.1-/-
G
Average rate of axonal growth (μm/hr)
5.00
4.50
4.00
3.50
3.00
2.50
2.00
1.50
1.00
0.50
0.00
WT
Nkx2.1 -/-
H
Distance from origin (μm)
600.00
500.00
400.00
300.00
200.00
100.00
0.00
***
WT
Nkx2.1 -/-

Figure 7. ***The MGE- and the CGE-derived GABAergic neurons exert attractive influence on callosal axons***

(A1) Experimental paradigm used to verify that transplantations in the septum don't cause callosal axon navigation defects. A small explant of the E16.5 GAD67-GFP+ septal region was transplanted into the septal region of the wild-type host. **(A2-A3)** DiI-labelled callosal axons continue to extend normally through the CC neurons without any diversions, thus, displaying the specificity of their orientation. Axons never penetrate the septum that constitutes a repulsive region.

(B1) *In vitro* model of organotypic slices to visualize if the CC neurons exert attractive influence on the callosal axons. A small explant of E16.5 GAD67-GFP+ CC containing GABAergic neurons is transplanted in the septal region of the wild-type host. **(B2-B3)** DiI-labelled callosal axons penetrate the septum towards the explant.

(C1) As a control, the E16.5 GAD67-GFP+ lateral ganglionic eminence **(LGE)** explants that do not generate the CC GABAergic neurons are transplanted into the septum of E16.5 slice. **(C2-C3)** The LGE explant doesn't attract callosal axons through the repulsive septal region.

(D1 and **E1)** Experimental paradigm used to determine the respective contribution of the MGE- **(D1)** or the CGE- **(E1)** derived GABAergic neurons to attract callosal axons. To estimate these effects, we placed small explants of E16.5 MGE **(D1-D3)** or E16.5 CGE **(E1-E3)** that both generate the CC GABAergic neurons into the non permissive septal region of E16.5 host slices. **(D2-D3** and **E2-E3)** DiI staining showing that numerous callosal axons penetrate through the septum and are attracted by GAD67-GFP^{+} migrating GABAergic interneurons derived from the MGE **(D3**, arrowheads**)** or the CGE **(E3**, arrowheads**)** transplants. Both neuronal populations are found to exert equivalent attractive activities. All sections were counterstained with Hoechst that labels cell nuclei in blue.

(F1-F4) Experimental paradigms used to determine whether the CC **(F1)** exerts attractive effects on cortical axons. **(F2)** Immunohistochemical staining for betaIII-tubulin on E16.5 frontal cortex **(CFr)** co-cultured with E16.5 GAD67-GFP+ CC. **(F3)** Immunohistochemical staining for betaIII-tubulin on E16.5 GAD67-GFP+. Interestingly, callosal axons were seen to leave the cortical explant that comprises GAD67-GFP+ GABAergic neurons.

(F4) Quantification of the axonal guidance responses to E16.5 CC explants comprising GAD67-GFP+ GABAergic neurons. Data are expressed as a P/D ratio, where P and D are the mean fluorescence ± SEM intensity in the quadrants proximal and distal to the CC or septum explants. ***significantly different with $p<0.001$. CC GABAergic neurons cause strong chemoattraction on frontal axons. **(CFr)** frontal cortex; **(IG)** induseum griseum; **(LV)** lateral ventricle; **(SEP)** septum.

Bar = 485 µm in A2, B2, C2, D2, E2, F2, F3; 240 µm in A3, B3, C3 and 120 µm in D3, E3.

E16.5 + 2DIV cultured brain slices

A1

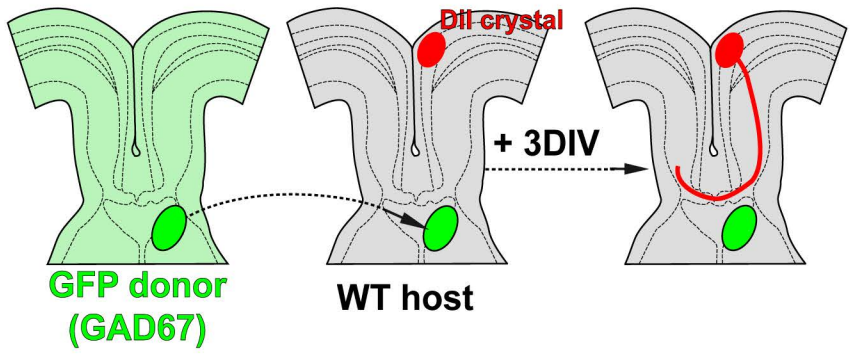

E16.5 SEP in E16.5 SEP+DiI

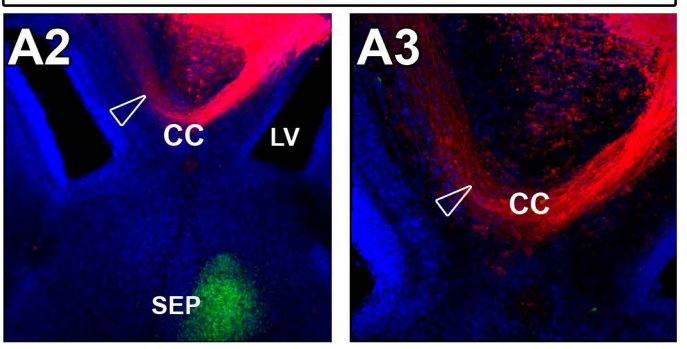

B1

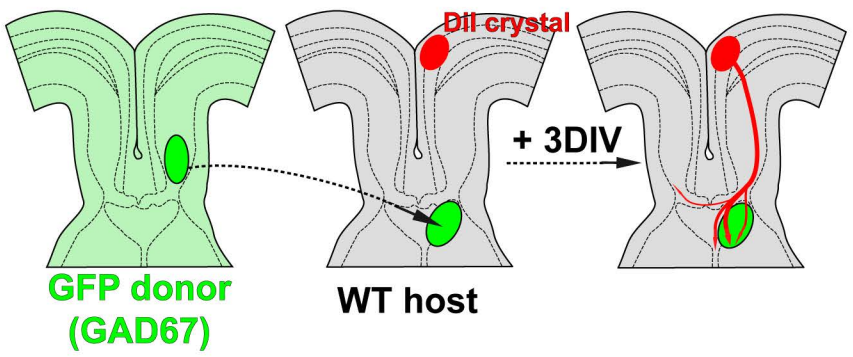

E16.5 CC in E16.5 SEP+DiI

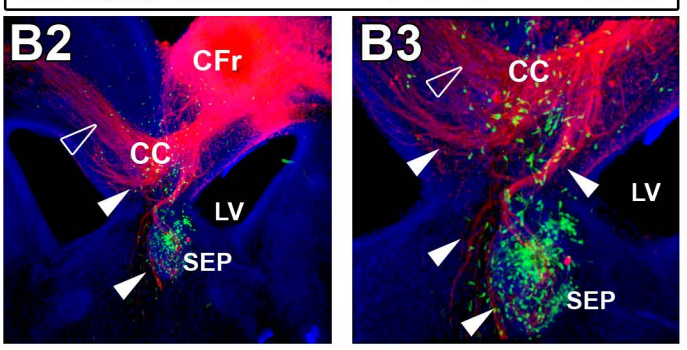

C1

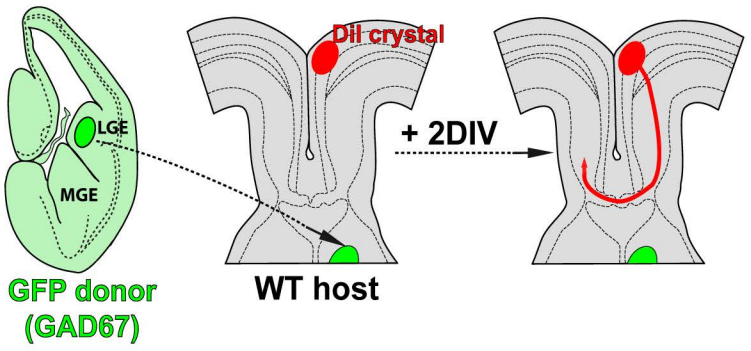

E16.5 LGE in E16.5 SEP+DiI

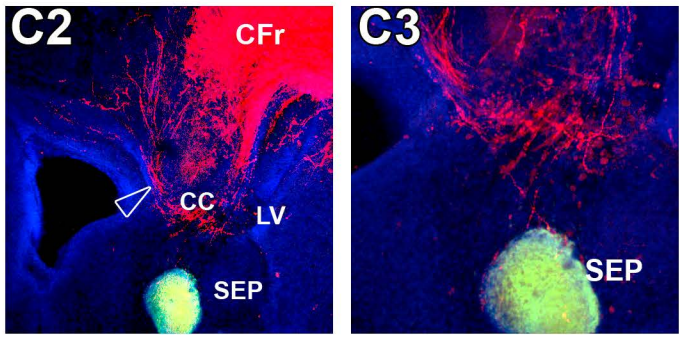

D1

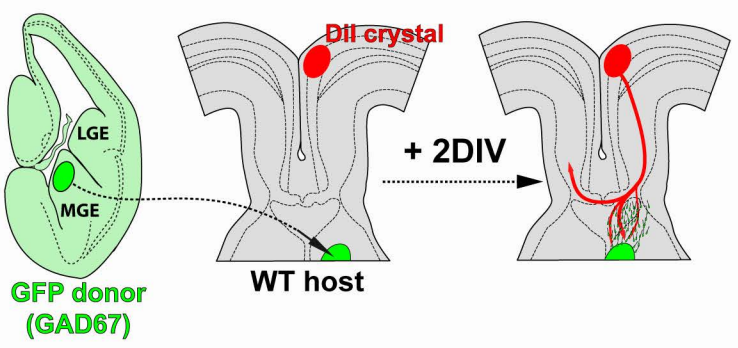

E16.5 MGE in E16.5 SEP+DiI

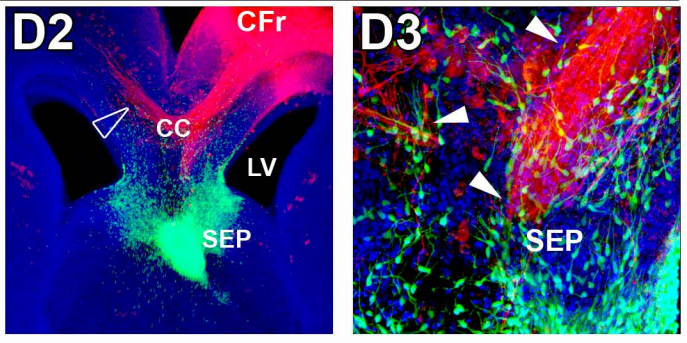

E1

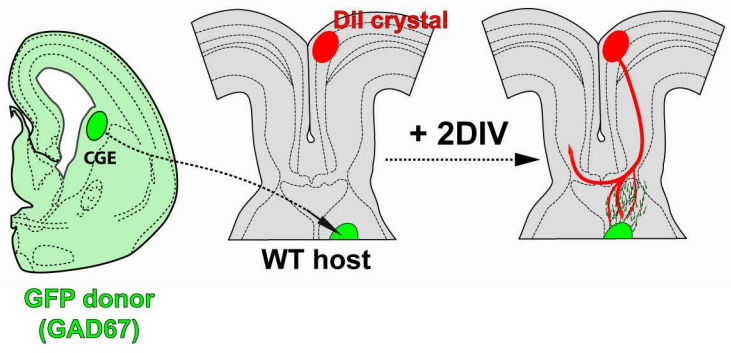

E16.5 CGE in E16.5 SEP+DiI

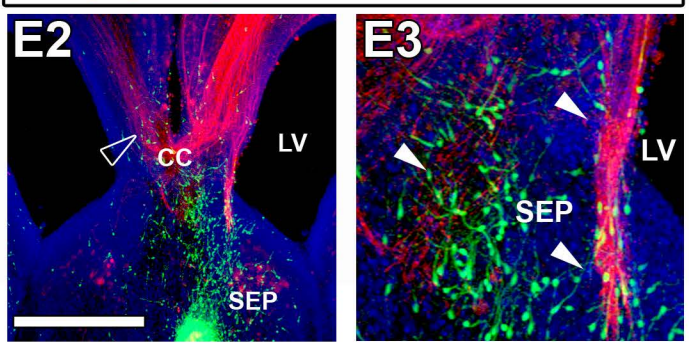

E16.5 Co-explants

E16.5 CFr↔E16.5 CC

F1

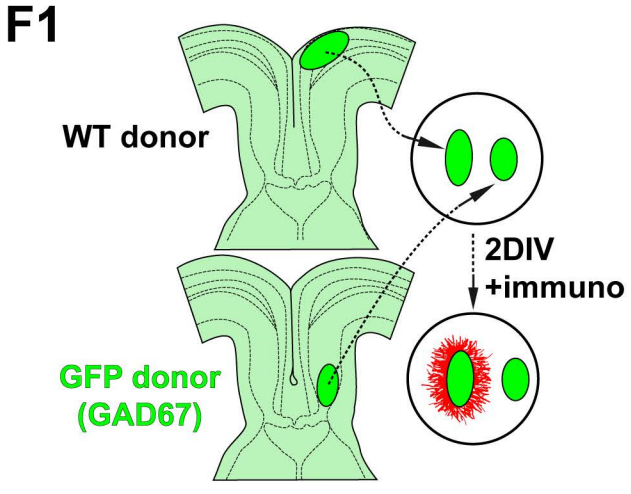

betaIII-tub/ GAD67GFP

F2

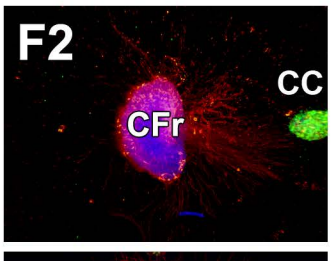

F3

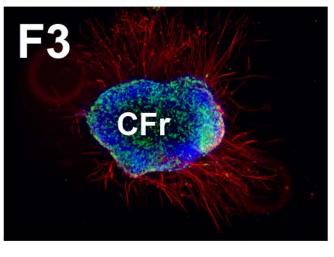

F4

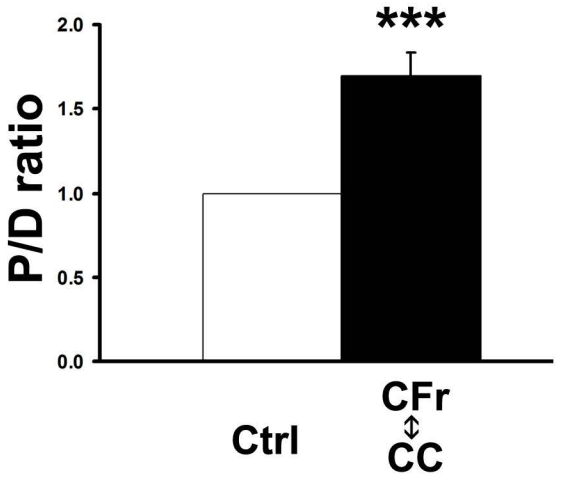

Figure 8. ***CC GABAergic neurons express short- and long-range guidance factors***
(A1-A3) Genetic screen for guidance factors expressed by GABAergic guidepost neurons. **(A1)** After microdissection, GABAergic neurons of the CC and of the bordering cortical area, labelled for GAD67-GFP, are isolated by FACS sorting and mRNAs for guidance cues are screened by a sensitive RT-PCR. The cDNA amplification and screen is performed in 6 steps: (1) the 300 GFP+ and 300 GFP- are isolated by FACS sorting, (2) the lysis of the sorted cells and the reverse transcription of total mRNA into cDNA are performed simultaneously, (3) the cDNA is precipitated, (4) the 3'-oligo(dA) tailing is done on precipitated cDNA, (5) the cDNAs are globally amplified by PCR, and (6) the genes for guidance cues are screened by PCR using specific primers. **(A2)** GAD67-GFP+ neurons (labelled as **R2**) corresponding to 11.5% of the total CC cells population are purified by flow cytometry. **(A3)** Expression profile of flow-cytometer sorted GFP+ and GFP- cell fractions ascertained with specific primers against the various cell makers and guidance cues of interest. Using primers for GAD67, we can verify the selectivity of the FACS sorting method since GFP+ neurons but not GFP- cells express GAD67. In accordance with the literature, the GFP- cells of the CC correspond to VGLUT+ and Tbr+ glutamatergic neurons, Emx2+ precursors and GFAP+ astrocytes or radial glia. Using selective primers for guidance cues, GAD67-GFP+ neurons are found to express several long range guidance cues or receptors (ephrinB1/B2/A1/A4 and EphA4/B2/B3, sema3A and Npn1/2) and adhesion molecules (NrCAM, NCAM1, NCadh).
(B1-G2) *In situ* hybridization for *ephrinB1* **(B1-B2)**, *ephrinB2* **(C1-C2)**, *EphB2* **(D1-D2)**, *EphA4* **(E1-E2)** and *Sema3A* **(F1-F2)** mRNAs combined with immunohistochemical staining for GFP in coronal telencephalon sections of E16.5 GAD67-GFP mice**. (G1-G2)** Double immunohistochemical staining for Npn-2 and GFP in coronal telencephalon sections of E15.5-E16.5 GAD67-GFP mice. **B2, C2, D2, E2, F2 and G2** are high power views of the CC seen in **B1**, **C1, D1, E1, F1 and G1 (**open arrows**)**. Consistent with the PCR results, in all the panels GAD67-GFP+ GABAergic neurons of the CC (arrowheads) and other cells (*) of the CC that are negative for the GFP express strong levels of respective mRNAs. GABAergic neurons are heterogeneous with respect to their expression of various guidance cues since certain GAD67-GFP+ neurons (arrowheads) but not all (open arrowheads) express *ephrinB1/B2*, *EphB2/A4*, *Sema3A* mRNAs and Npn-2 (shown here).
Bar = 435 µm in B1, C1, D1, E1, F1, G1; 40 µm in B2, C2, D2, F2 and 20 µm in E2, G2.

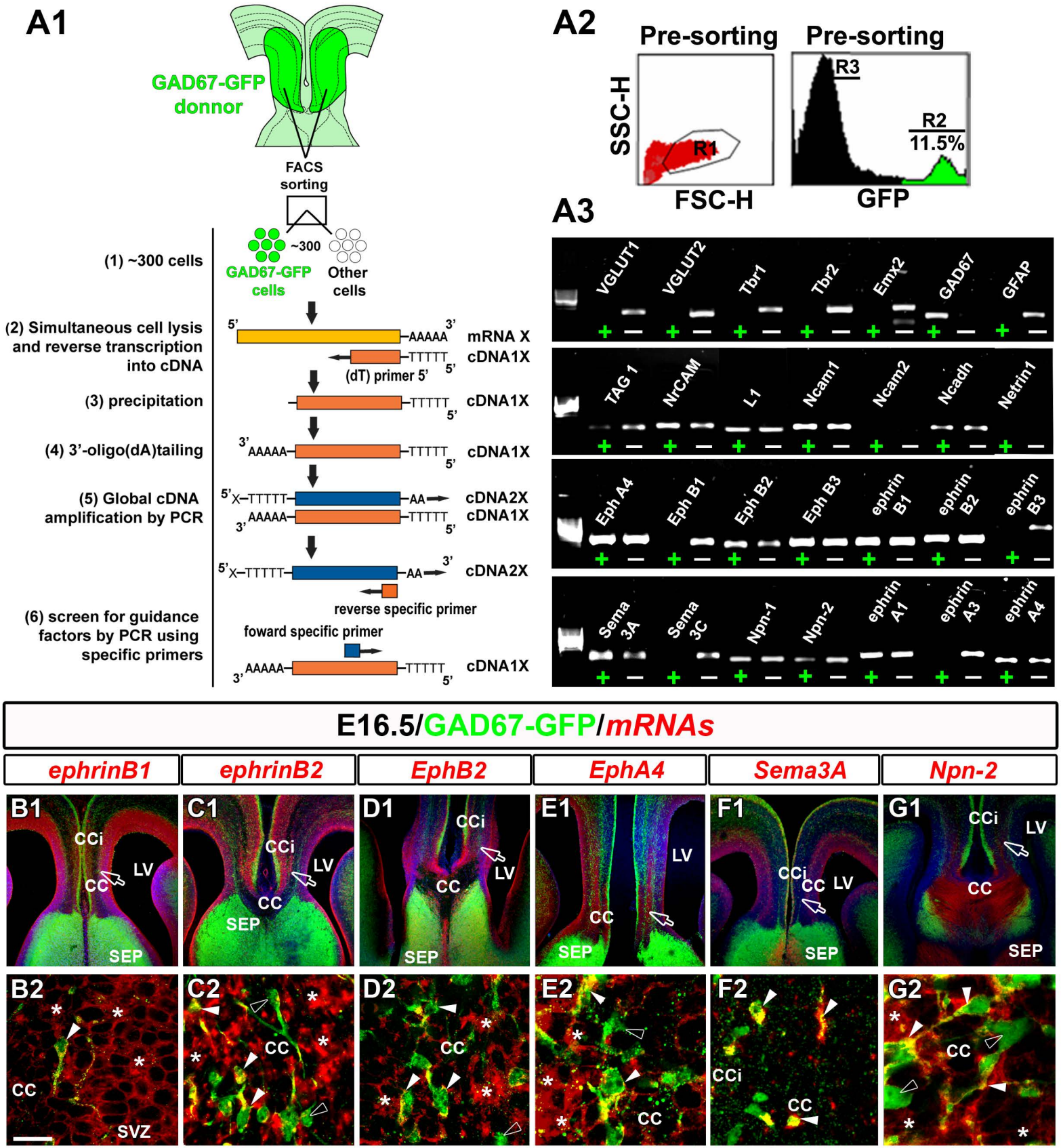
A1
GAD67-GFP donnor
FACS sorting
~300
GAD67-GFP cells
Other cells
(1) ~300 cells
(2) Simultaneous cell lysis and reverse transcription into cDNA
mRNA X
cDNA1X
(dT) primer 5'
(3) precipitation
cDNA1X
(4) 3'-oligo(dA)tailing
cDNA1X
(5) Global cDNA amplification by PCR
cDNA2X
cDNA1X
cDNA2X
reverse specific primer
(6) screen for guidance factors by PCR using specific primers
foward specific primer
cDNA1X
A2
Pre-sorting
Pre-sorting
SSC-H
FSC-H
R1
R3
R2
11.5%
GFP
A3
VGLUT1
VGLUT2
Tbr1
Tbr2
Emx2
GAD67
GFAP
TAG 1
NrCAM
L1
Ncam1
Ncam2
Ncadh
Netrin1
Eph A4
Eph B1
Eph B2
Eph B3
ephrin B1
ephrin B2
ephrin B3
Sema 3A
Sema 3C
Npn-1
Npn-2
ephrin A1
ephrin A3
ephrin A4
E16.5/GAD67-GFP/mRNAs
ephrinB1
ephrinB2
EphB2
EphA4
Sema3A
Npn-2
B1
C1
D1
E1
F1
G1
CCi
LV
CC
SEP
B2
C2
D2
E2
F2
G2
SVZ

Supplementary Figure 1. ***MGE- and CGE-derived GABAergic precursors give birth each to half of the CC GABAergic neurons, accounting together for all CC GABAergic neurons***

(A and **B)** Graphs represent the comparison of neuronal density at E16.5 **(A)** and E18.5 **(B)** between MGE-derived Lhx6-GFP$^+$ **(**Lhx6**)**, LGE/CGE-derived Venus$^+$ **(**Venus**)** and CGE-derived *5-HTR3a*-GFP$^+$ **(**5-HTR3a**)** neurons in the medial **(**mid**)**, lateral **(**lat**)** and entire **(**tot**)** CC of *Lhx6-Cre/R26R-YFP, Nkx2.1-Cre/Dlx1-Venus^{fl}* and *5-HTR3a-GFP* mice, respectively. **(C** and **D**) Graphs represent the comparison between densities at E16.5 **(C)** and E18.5 **(D)** between the MGE$^+$ LGE/CGE-derived **(**Lhx6$^+$ Venus**)** neurons, the MGE$^+$ CGE-derived **(**Lhx6$^+$ 5-HTR3a**)** neurons and all GABAergic neurons labelled for GAD67-GFP in the medial **(**mid**)**, lateral **(**lat**)** and entire **(**tot**)** CC.

Comparison between density values were made at E16.5 and at E18.5 in similar portions of the CC using a *t*-test. After making the quantification at E16.5 and E18.5, the GABAergic neurons of the medial and the entire CC at both ages are found to be generated in equal proportion by the MGE and the LGE/CGE. The CGE however generates higher proportion of GABAergic neurons in the lateral CC compared to the MGE **(A** and **B,*)**. The values for the density of CC 5-HTR3a-GFP$^+$ neurons originating specifically from the CGE and of CC LGE/CGE-derived Venus$^+$ neurons are not significantly different **(A** and **B)** suggesting that CC GABAergic neurons originate from the MGE and the CGE but not the LGE. Finally, the comparison of the global neuronal population originating from both the MGE and the CGE with the GAD67-GFP$^+$ population **(C** and **D)** indicates that the MGE- and CGE-derived populations together generate the whole population of CC GABAergic guidepost neurons.

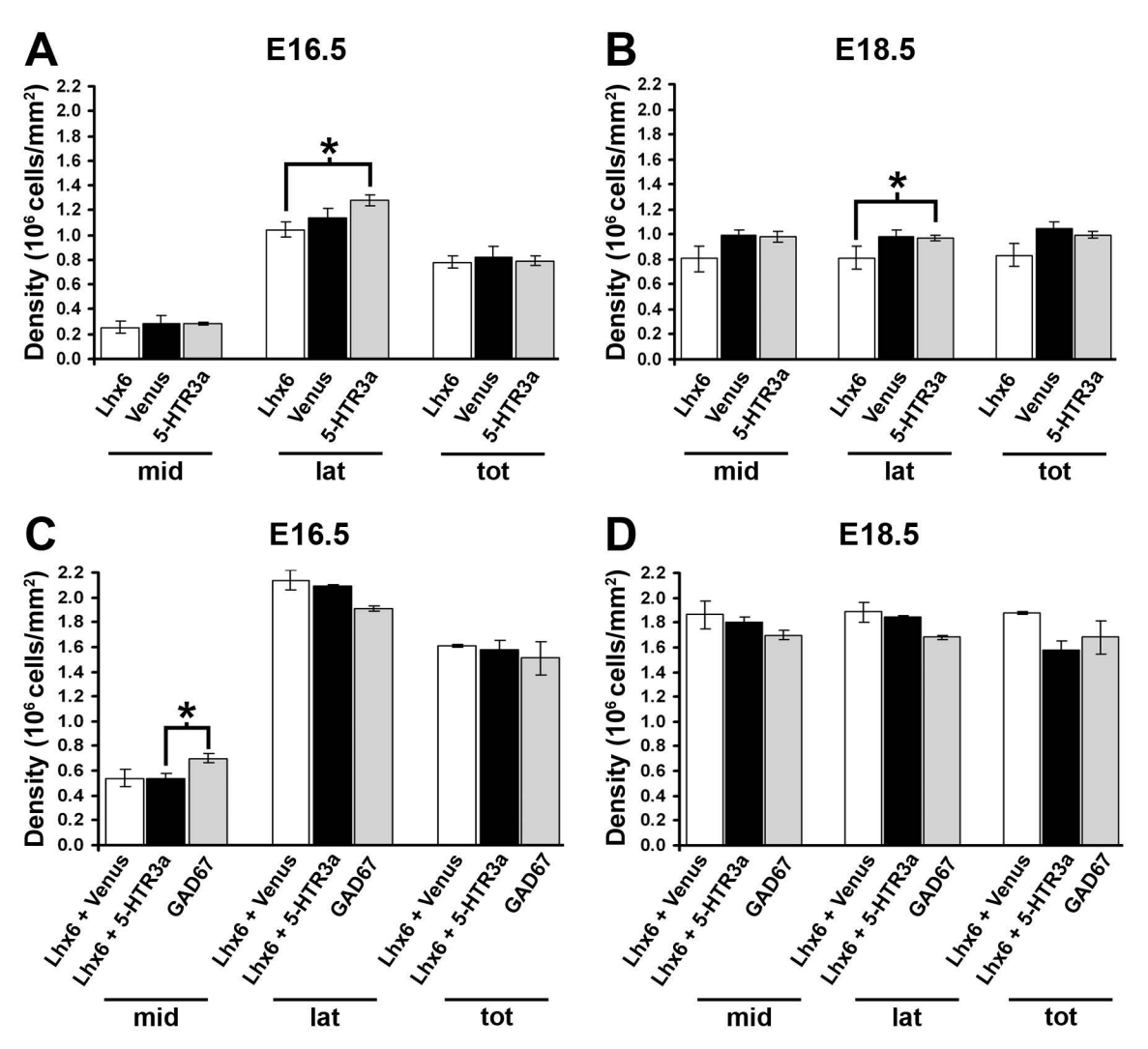
A
E16.5
B
E18.5
C
E16.5
D
E18.5
Density (10⁶ cells/mm²)
0.0
0.2
0.4
0.6
0.8
1.0
1.2
1.4
1.6
1.8
2.0
2.2
*
Lhx6
Venus
5-HTR3a
Lhx6 + Venus
Lhx6 + 5-HTR3a
GAD67
mid
lat
tot